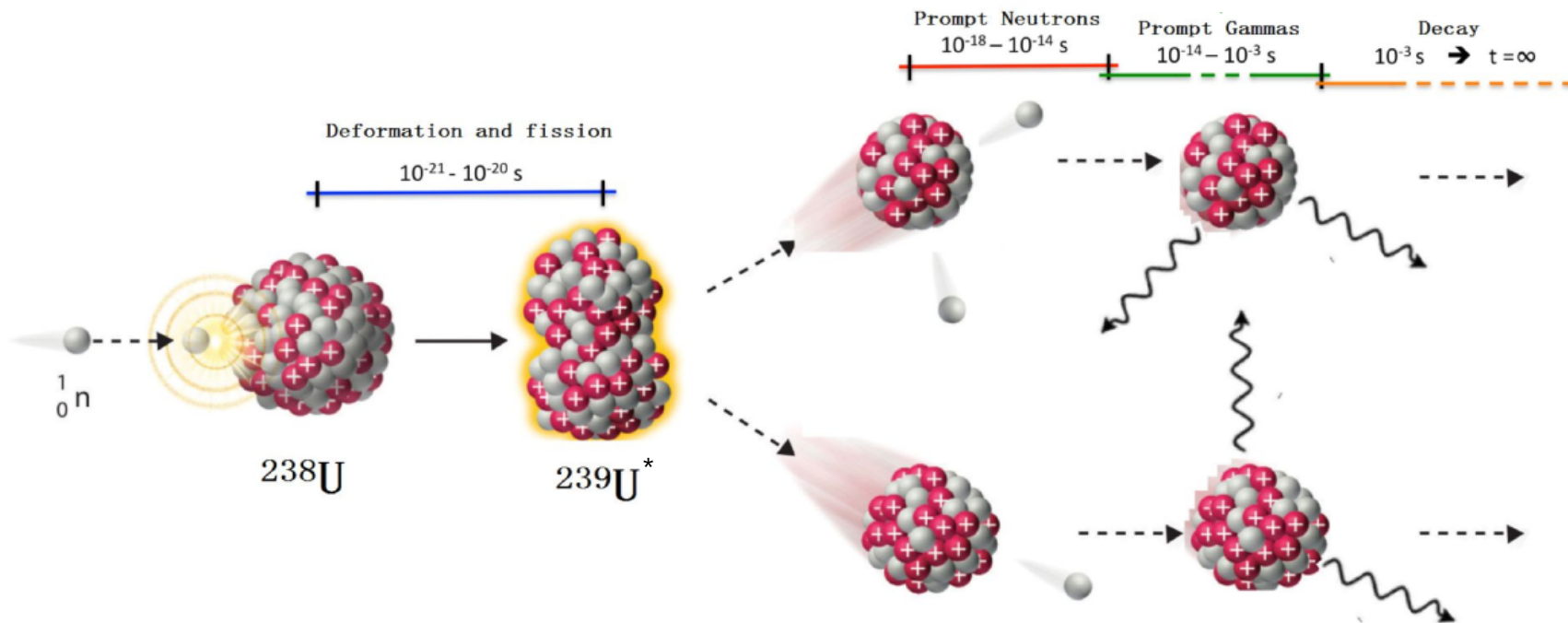




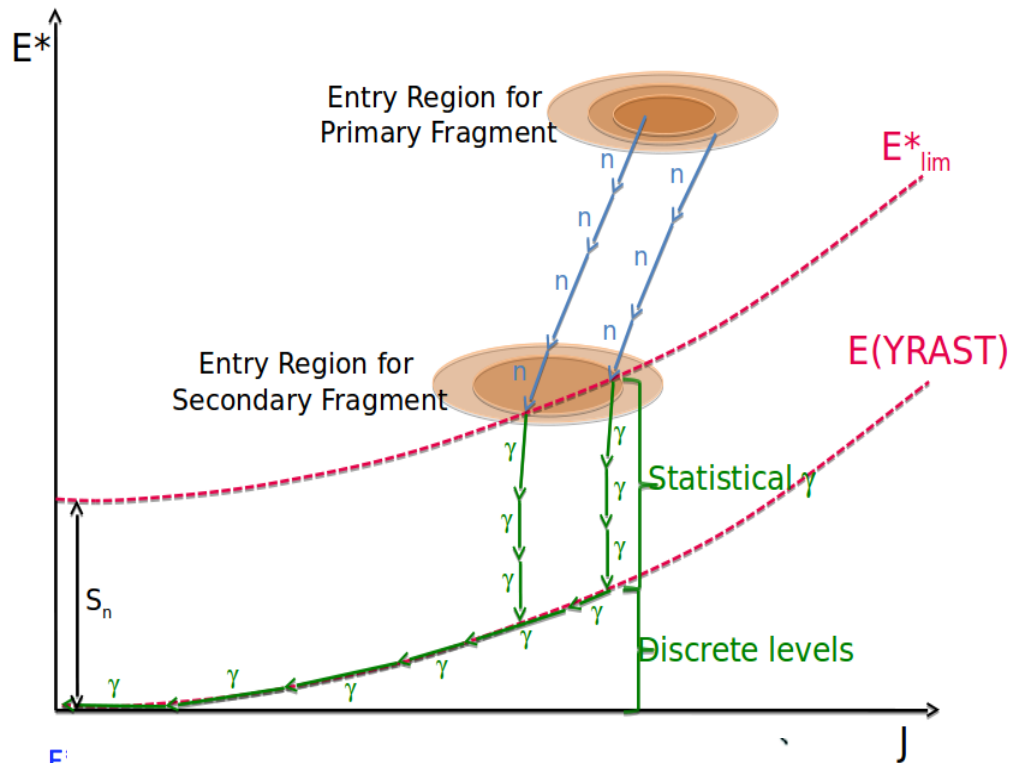
The Study of Gamma Emission in the Fission Process

Liqiang QI, Matthieu LEBOIS, Jonathan WILSON

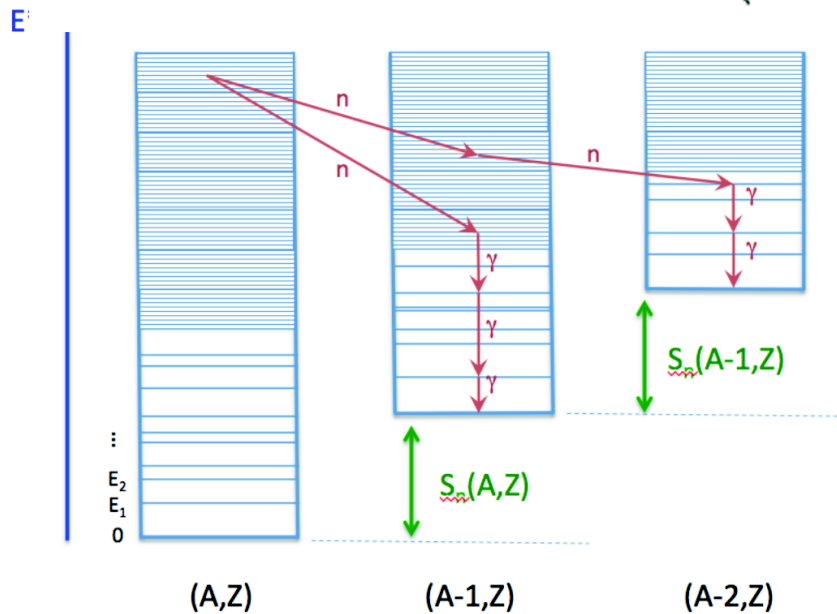
Group NESTER, Institut de Physique Nucléaire Orsay

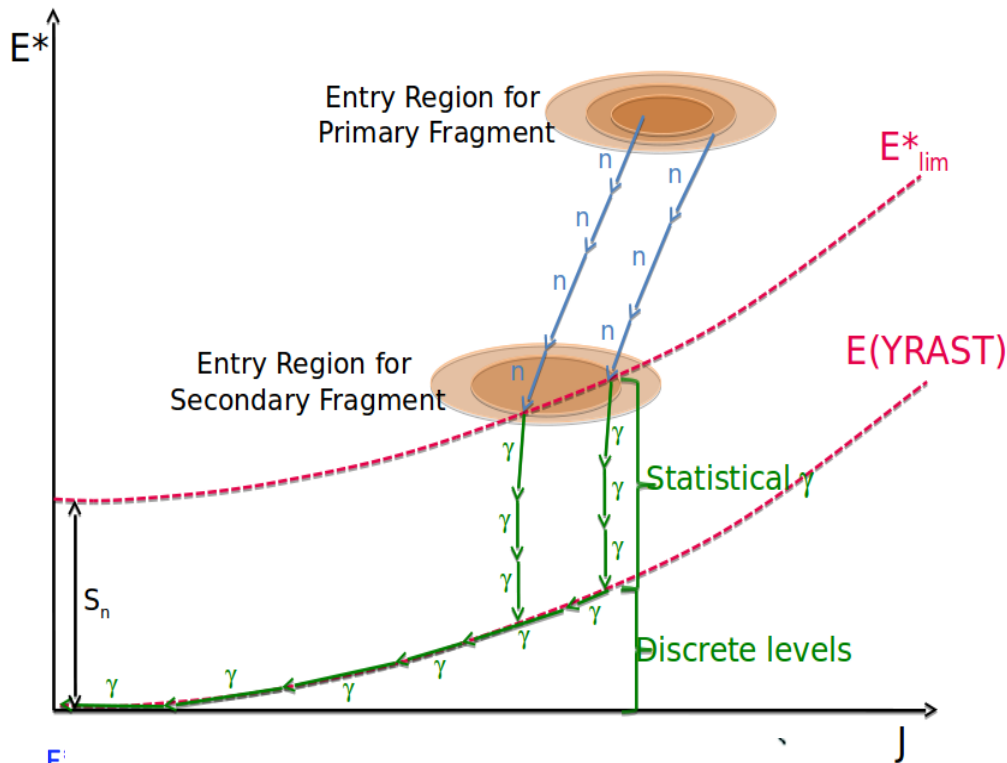


$$\begin{aligned}
 Q^* &= \text{TKE}^* + \text{TXE} \\
 \langle Q^* \rangle &\sim 196 \text{ MeV} \\
 \langle \text{TKE}^* \rangle &\sim 171 \text{ MeV} \\
 \langle \text{TXE} \rangle &\sim 25 \text{ MeV}
 \end{aligned}$$

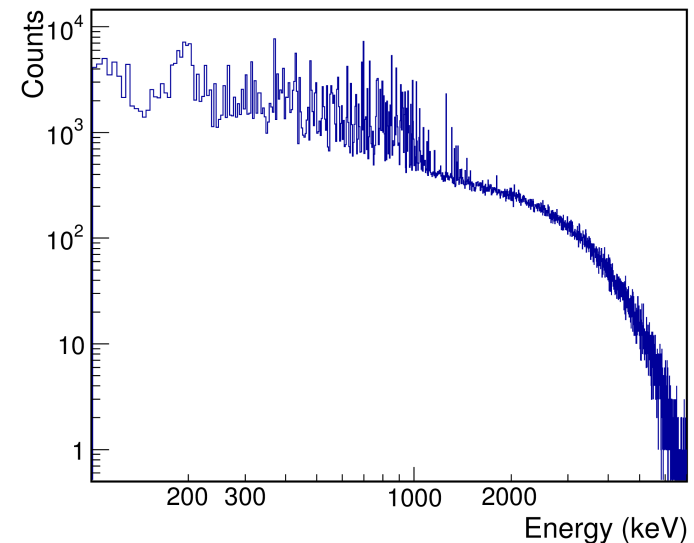
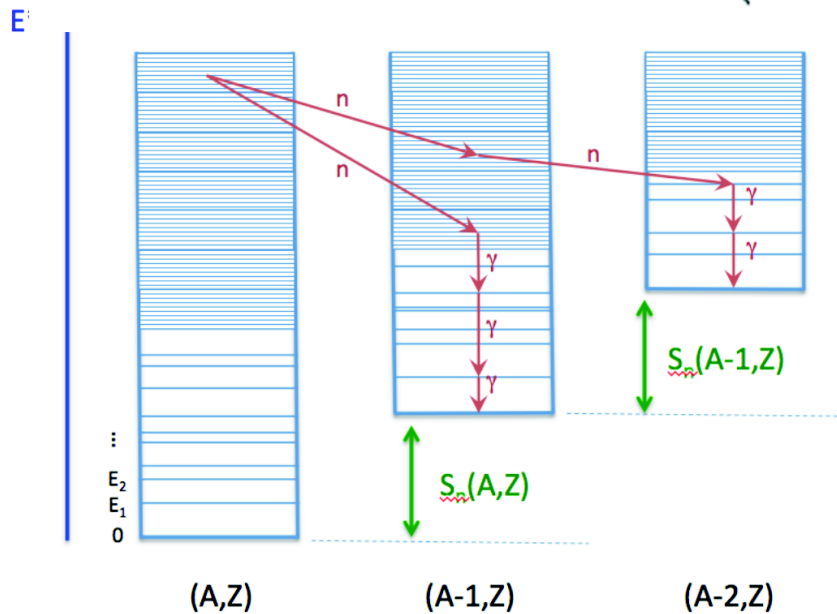


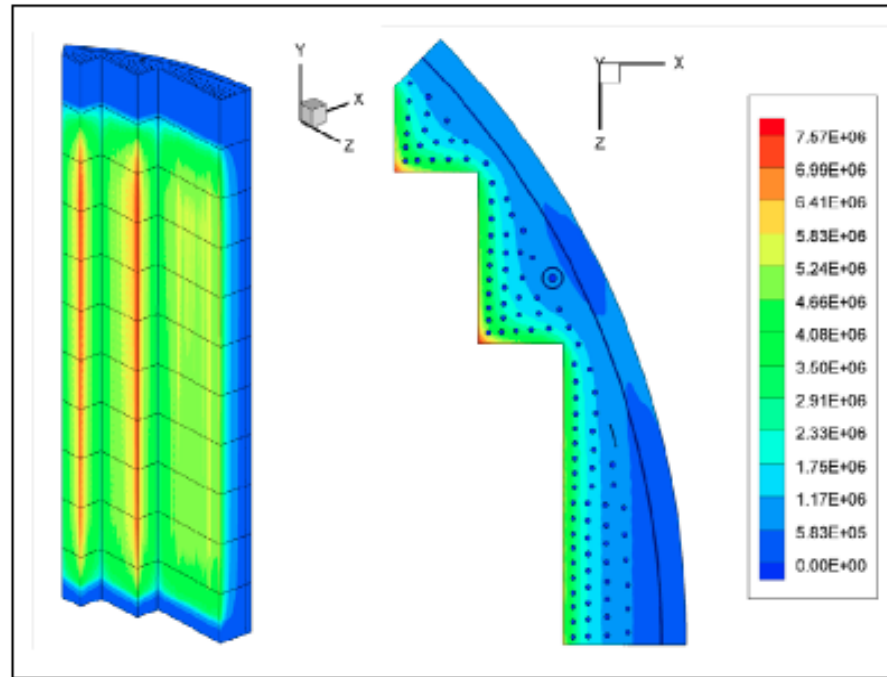
- 1. Energy partition in fission
- 2. Angular momentum generation
- 3. Competition between neutron and gamma ray emission
- 4. Nuclear structure information





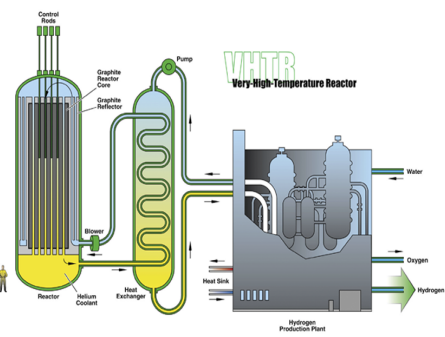
- 1. Energy partition in fission
- 2. Angular momentum generation
- 3. Competition between neutron and gamma ray emission
- 4. Nuclear structure information



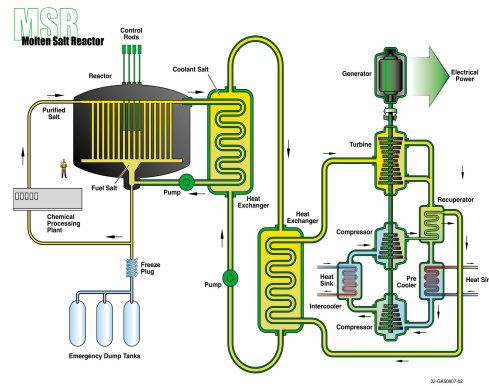


- Prompt Fission Gamma Spectrum (PFGS):
 - total energy, mean energy, multiplicity
- Gamma heating is underestimated up to 28%

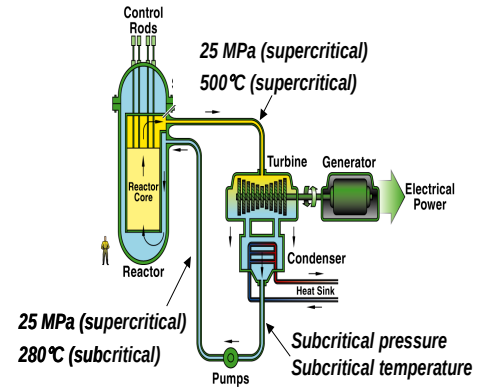
Thermal reactors



Very-high-temperature reactor (VHTR)

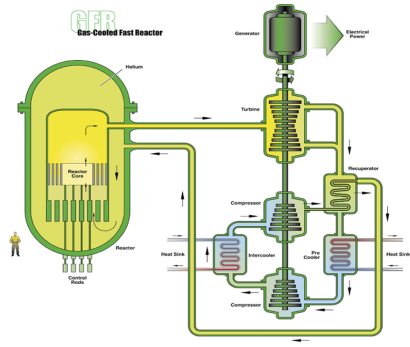


Molten-salt reactor (MSR)

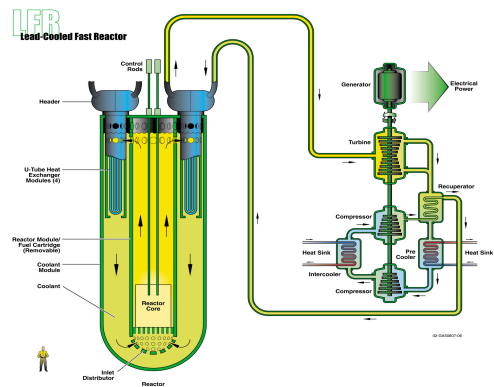


Supercritical-water-cooled reactor (SCWR)

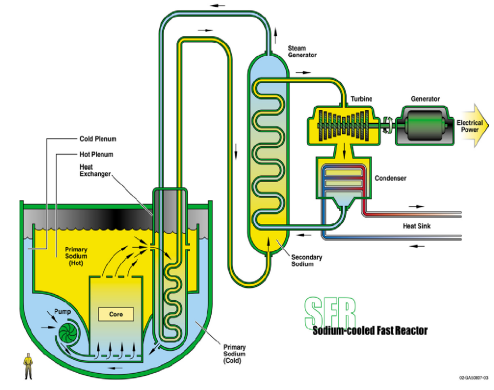
Fast reactors



Gas-cooled faster reactor (GFR)

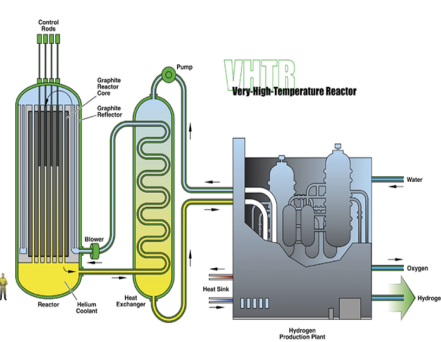


Lead-cooled faster reactor (LFR)

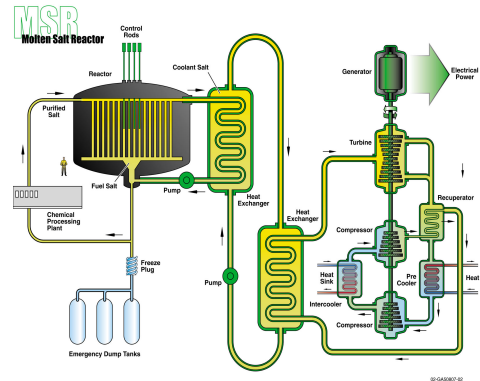


Sodium-cooled faster reactor (SFR)

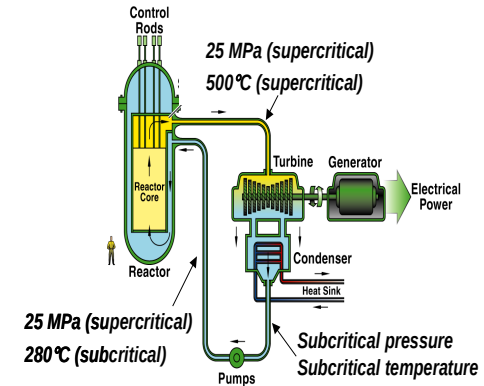
Thermal reactors



Very-high-temperature reactor (VHTR)

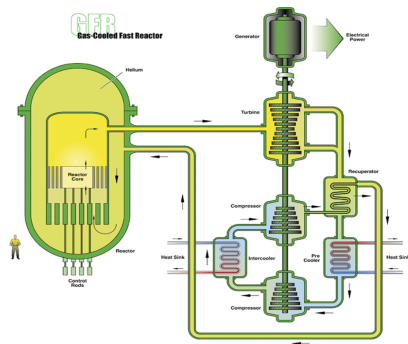


Molten-salt reactor (MSR)

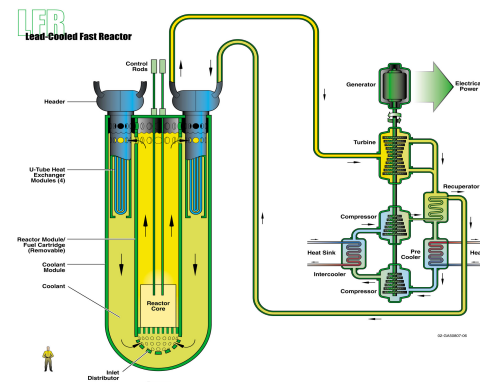


Supercritical-water-cooled reactor (SCWR)

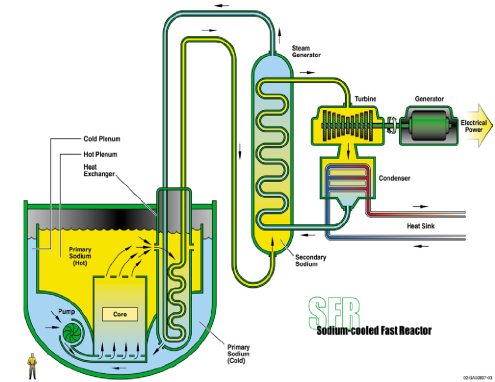
Fast reactors



Gas-cooled faster reactor (GFR)



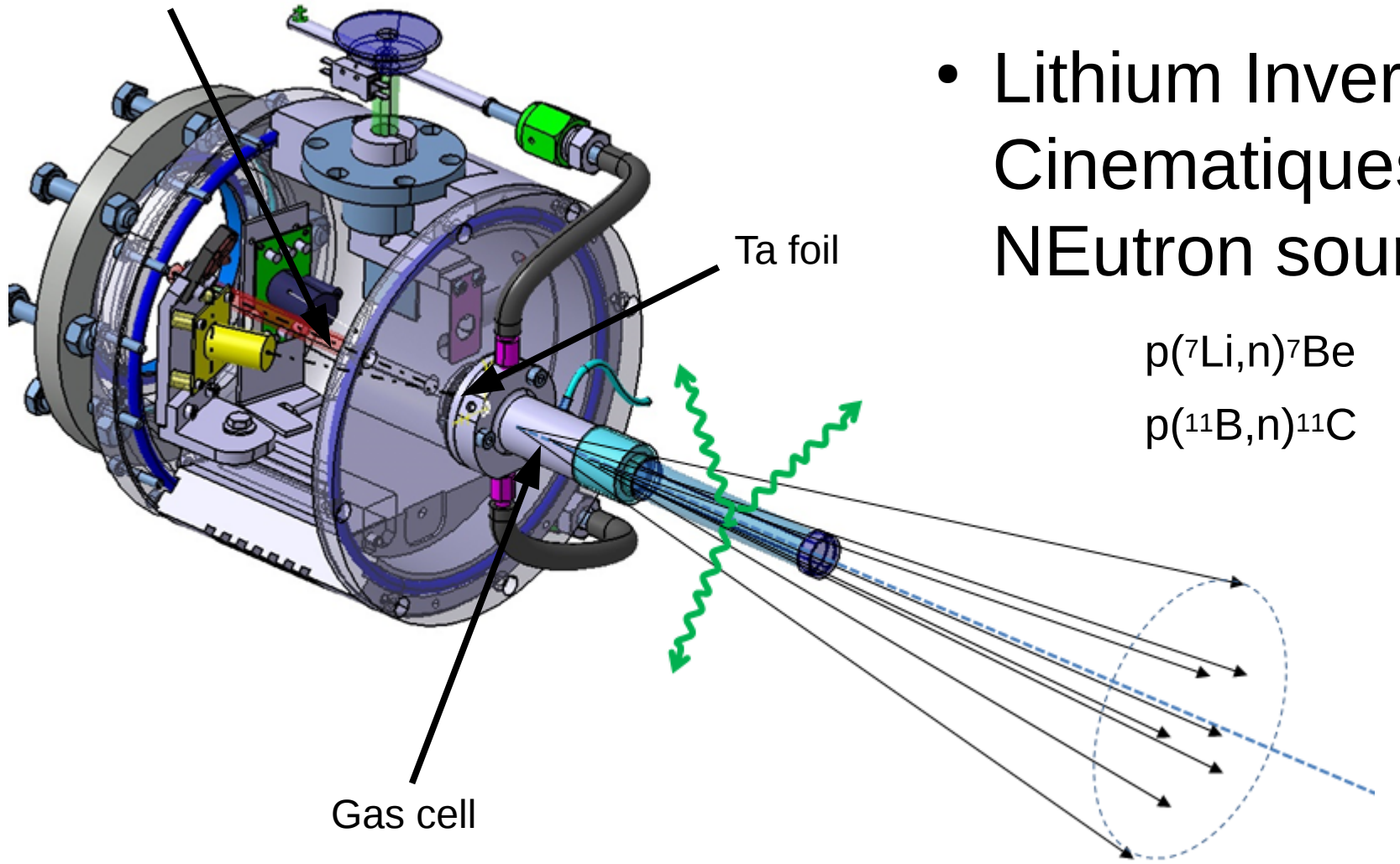
Lead-cooled faster reactor (LFR)



Sodium-cooled faster reactor (SFR)

$^{238}\text{U}(n, f)$ in fast neutron energy of 2.0 MeV and 4.6 MeV

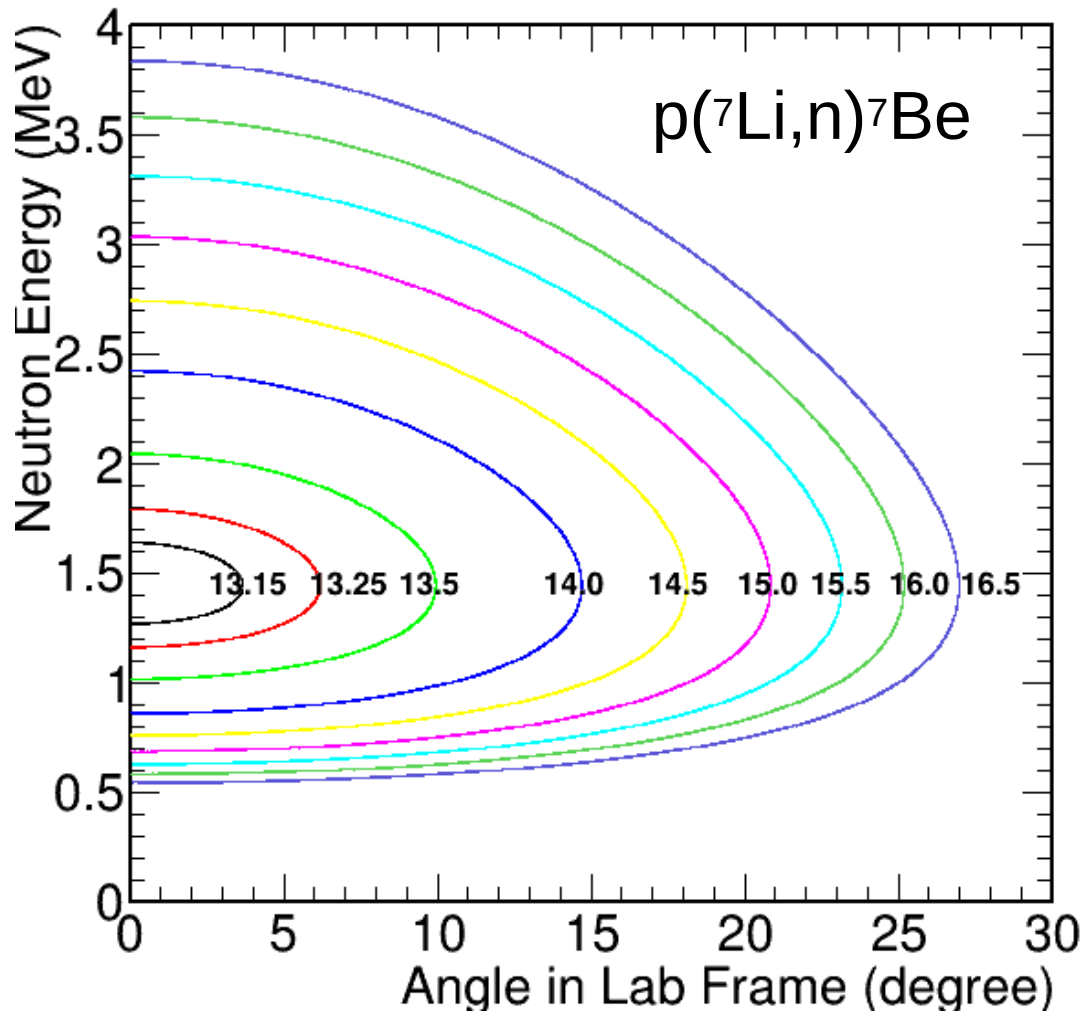
Pulsed beam
Or continuous beam

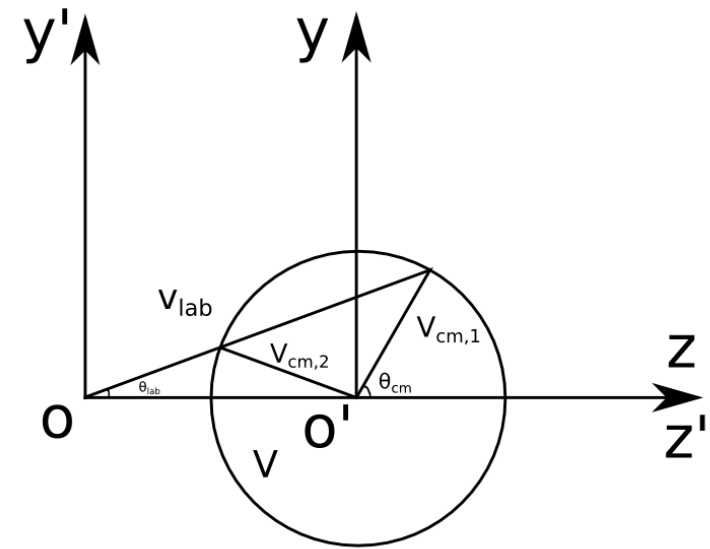
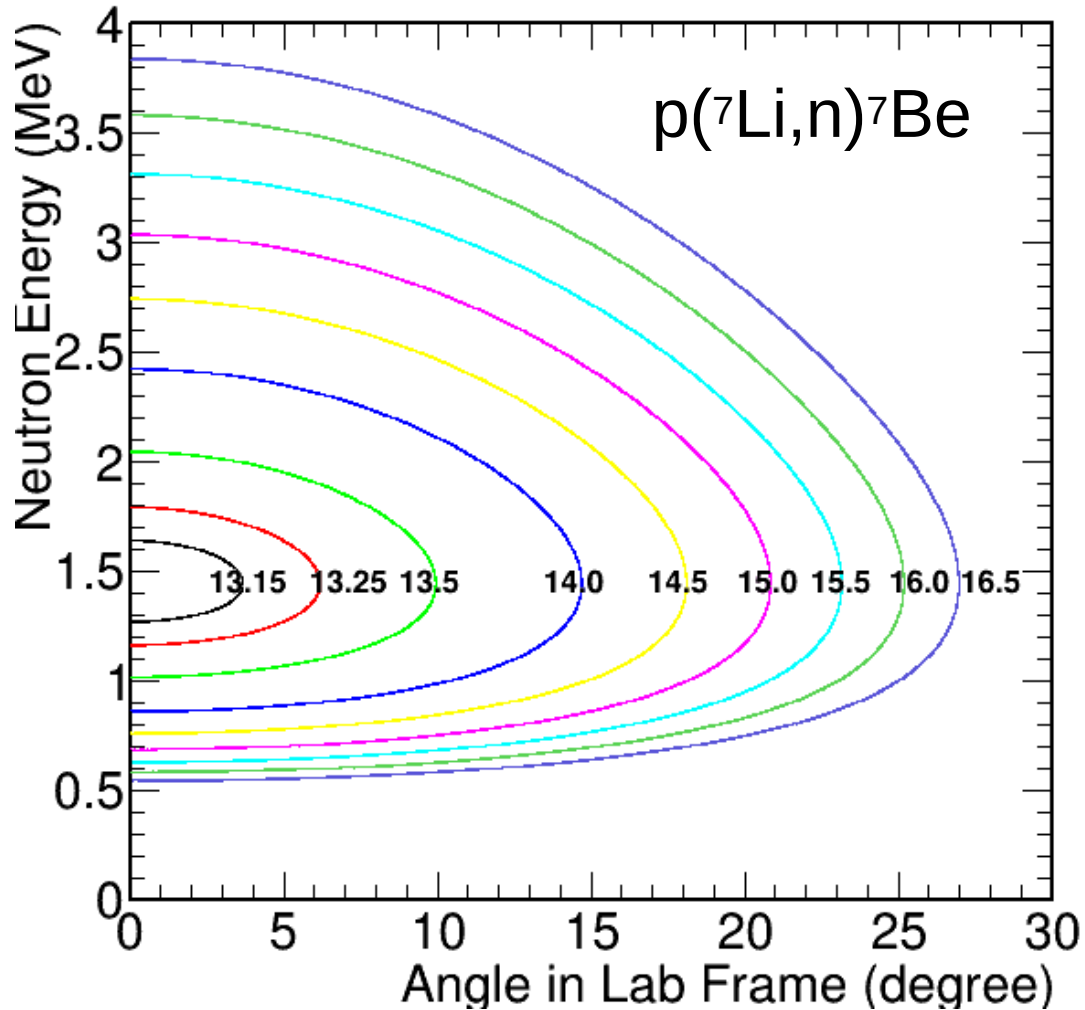


- Lithium Inverse Cinematiques ORsay NEutron source

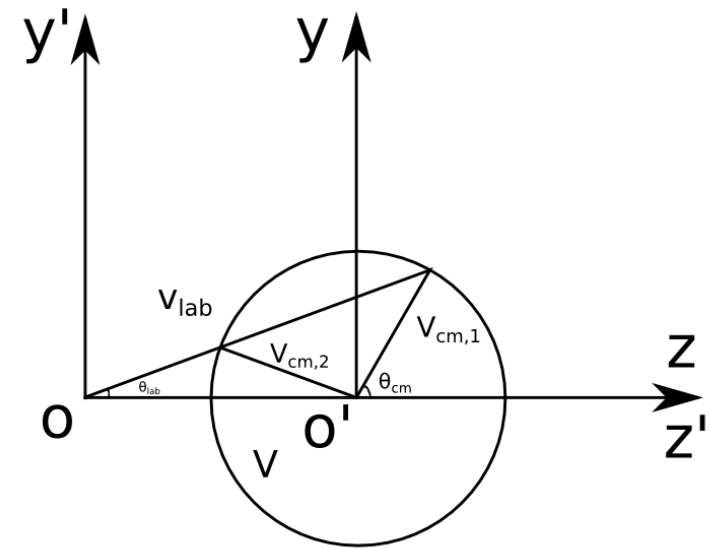
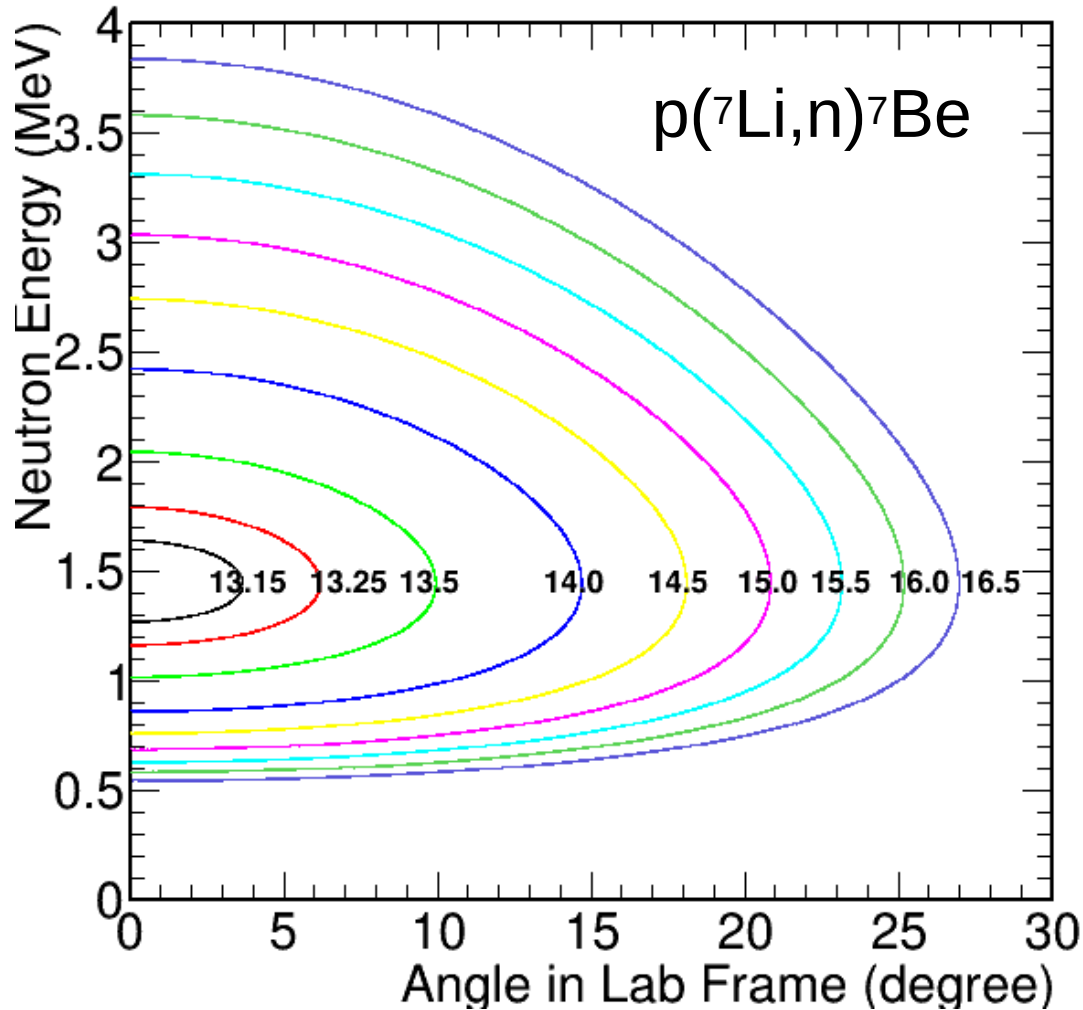


Cone opening up to 25°

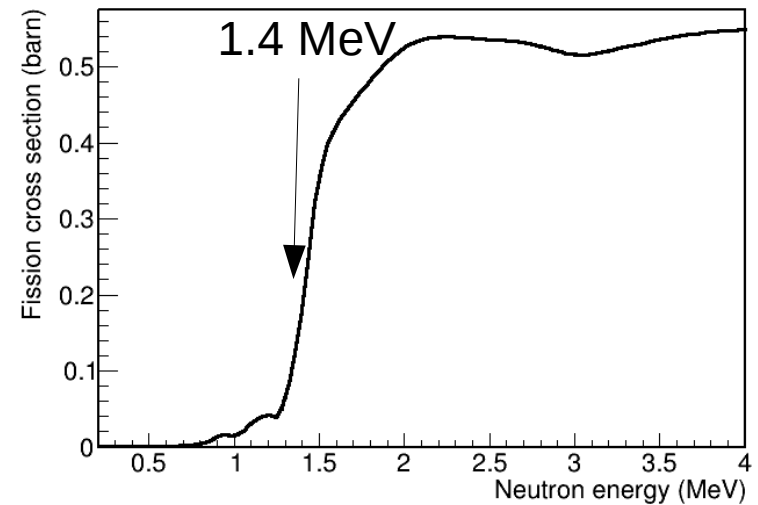




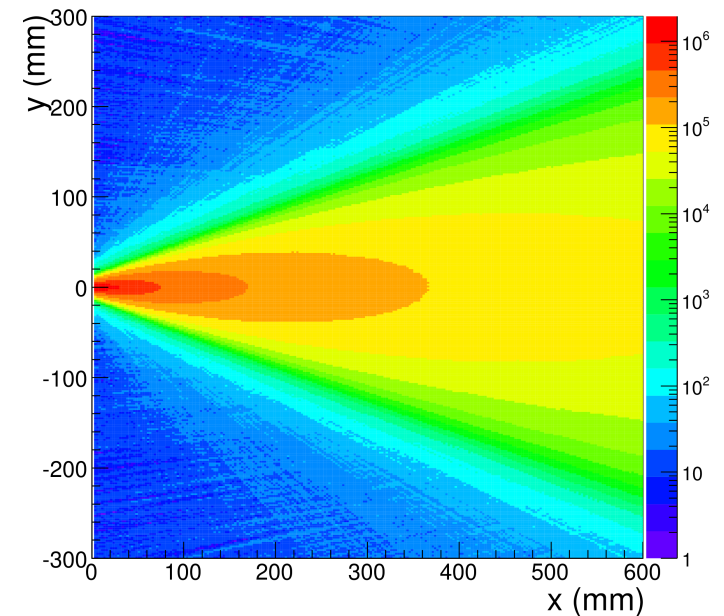
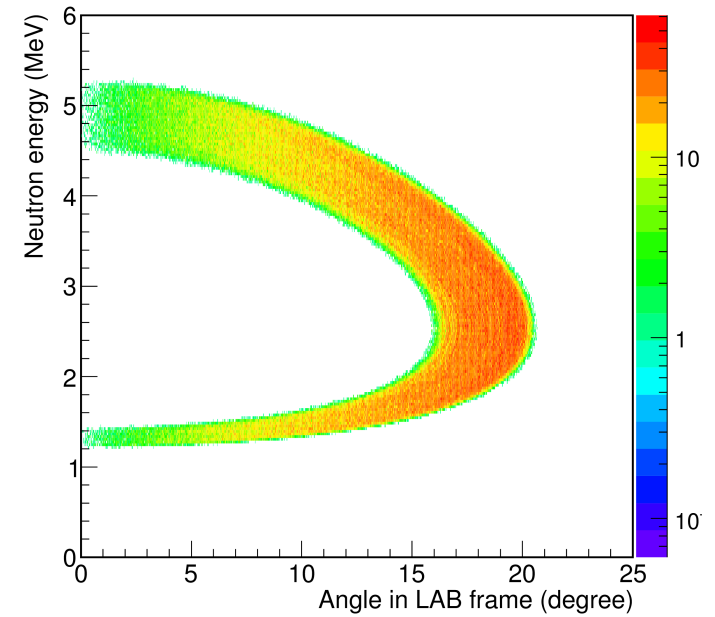
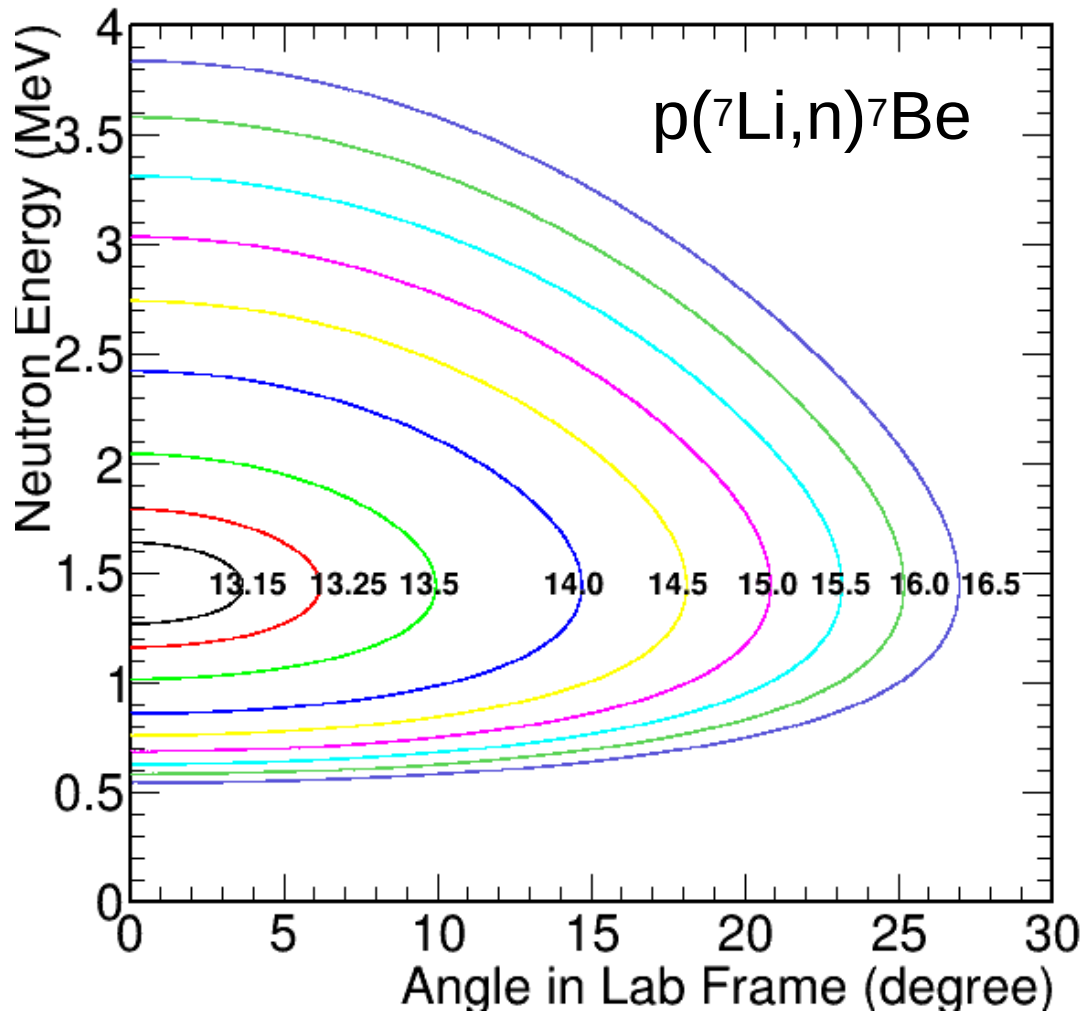
Inverse Kinematics

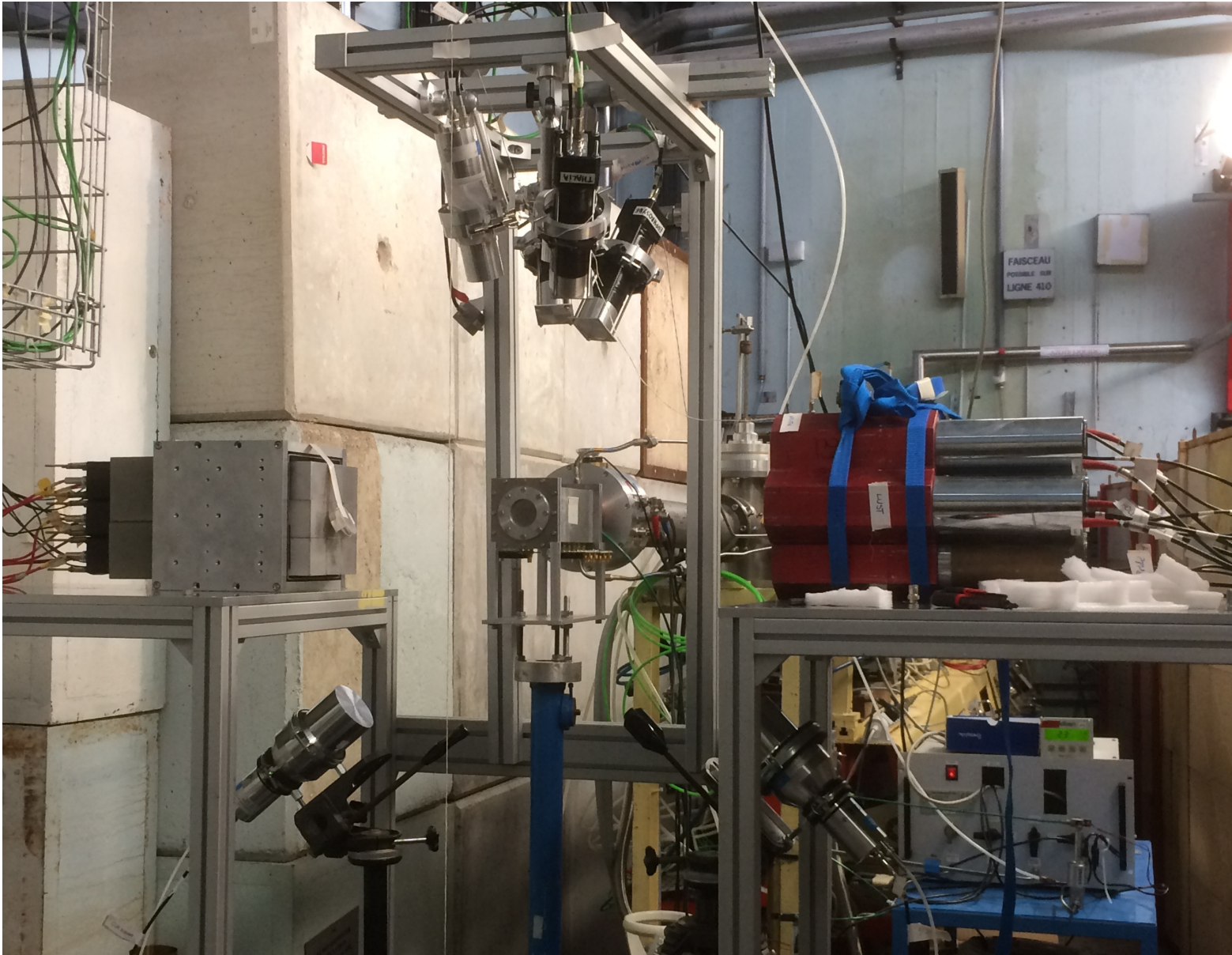


Inverse Kinematics



Fission cross section of ^{238}U
ENDF/B-VII.1

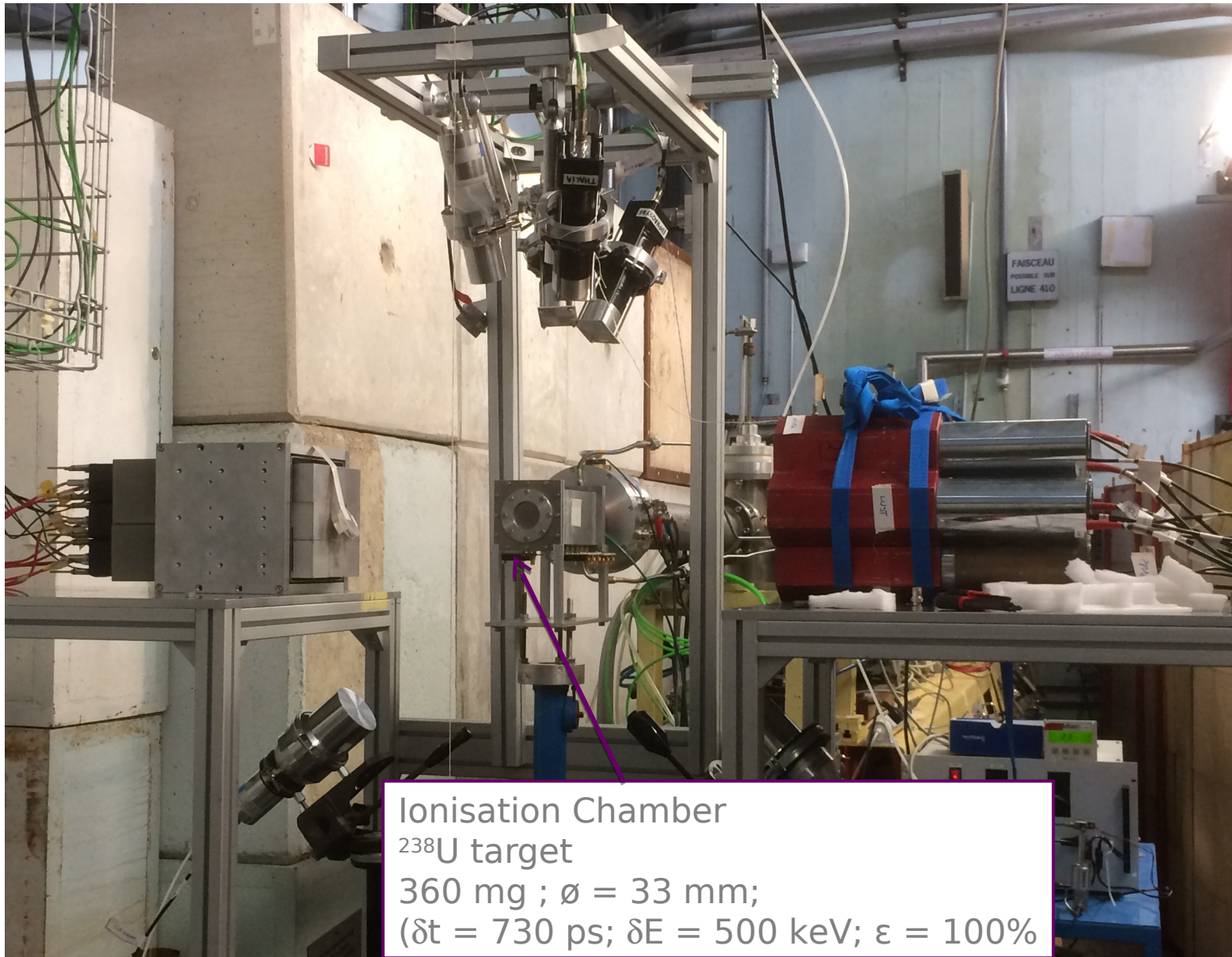


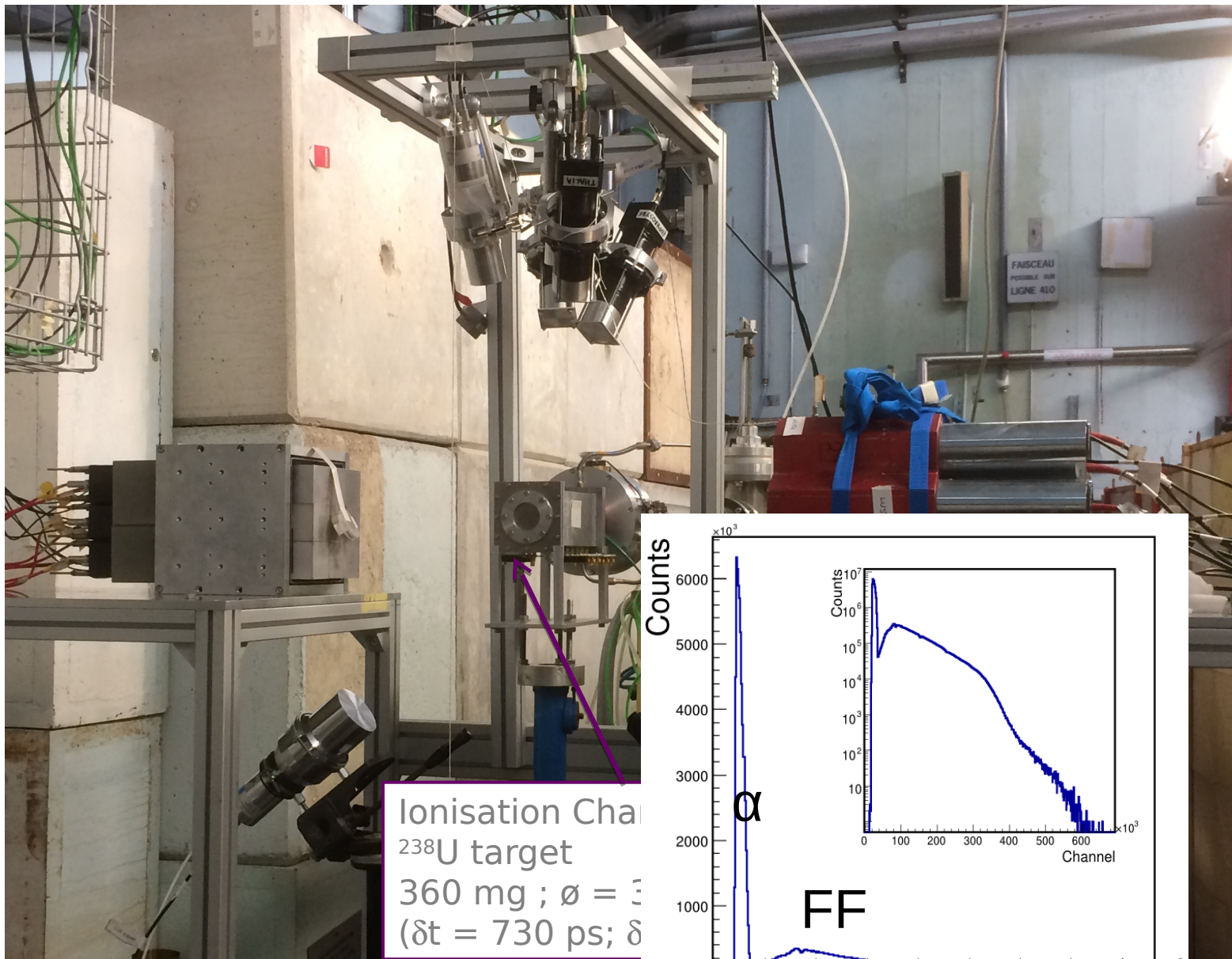


May 29, 2017

L. QI IPNO

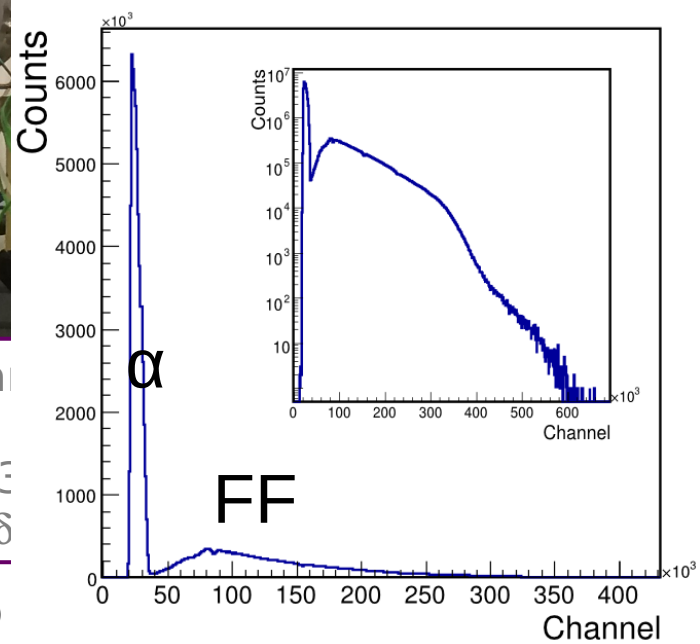
13



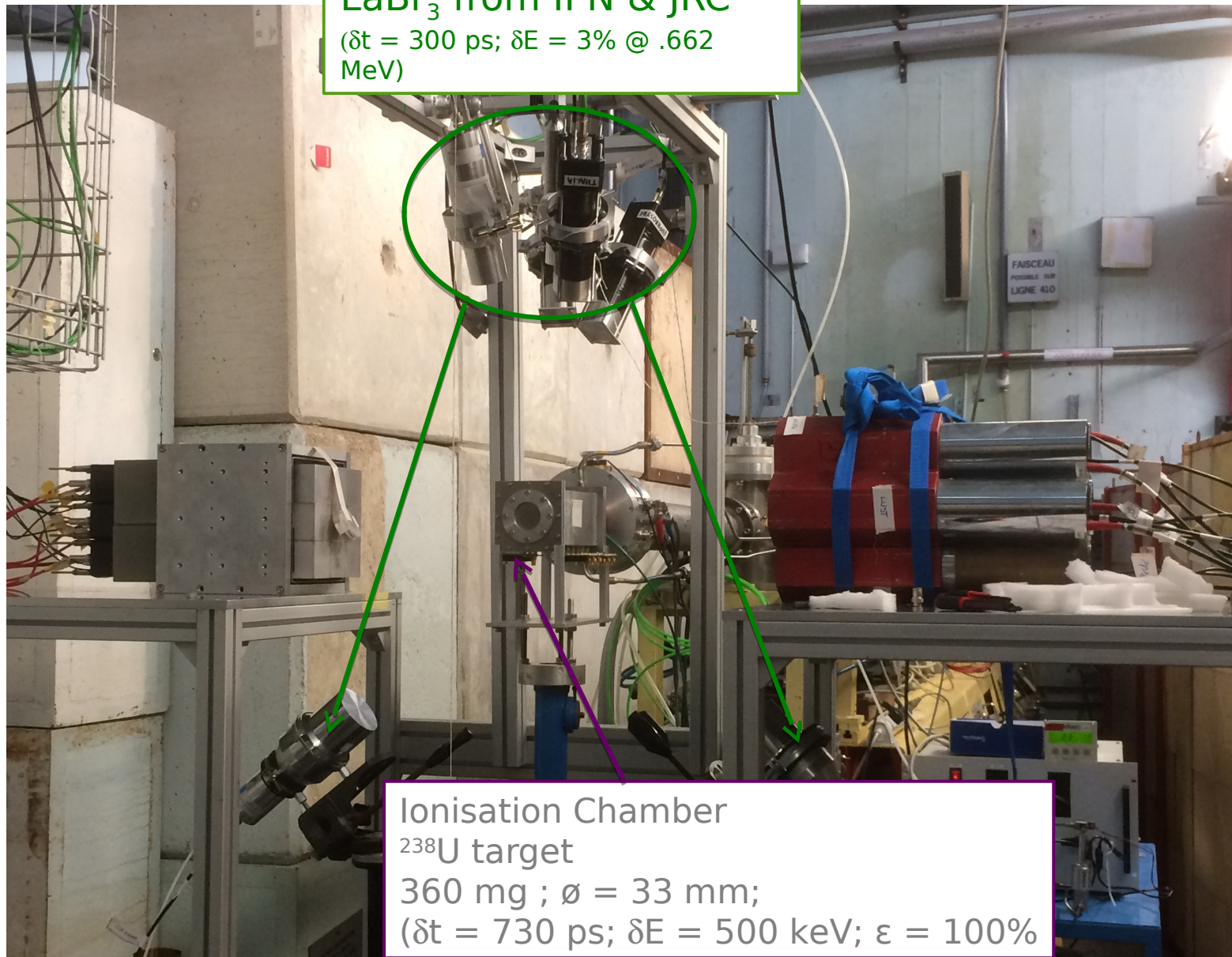


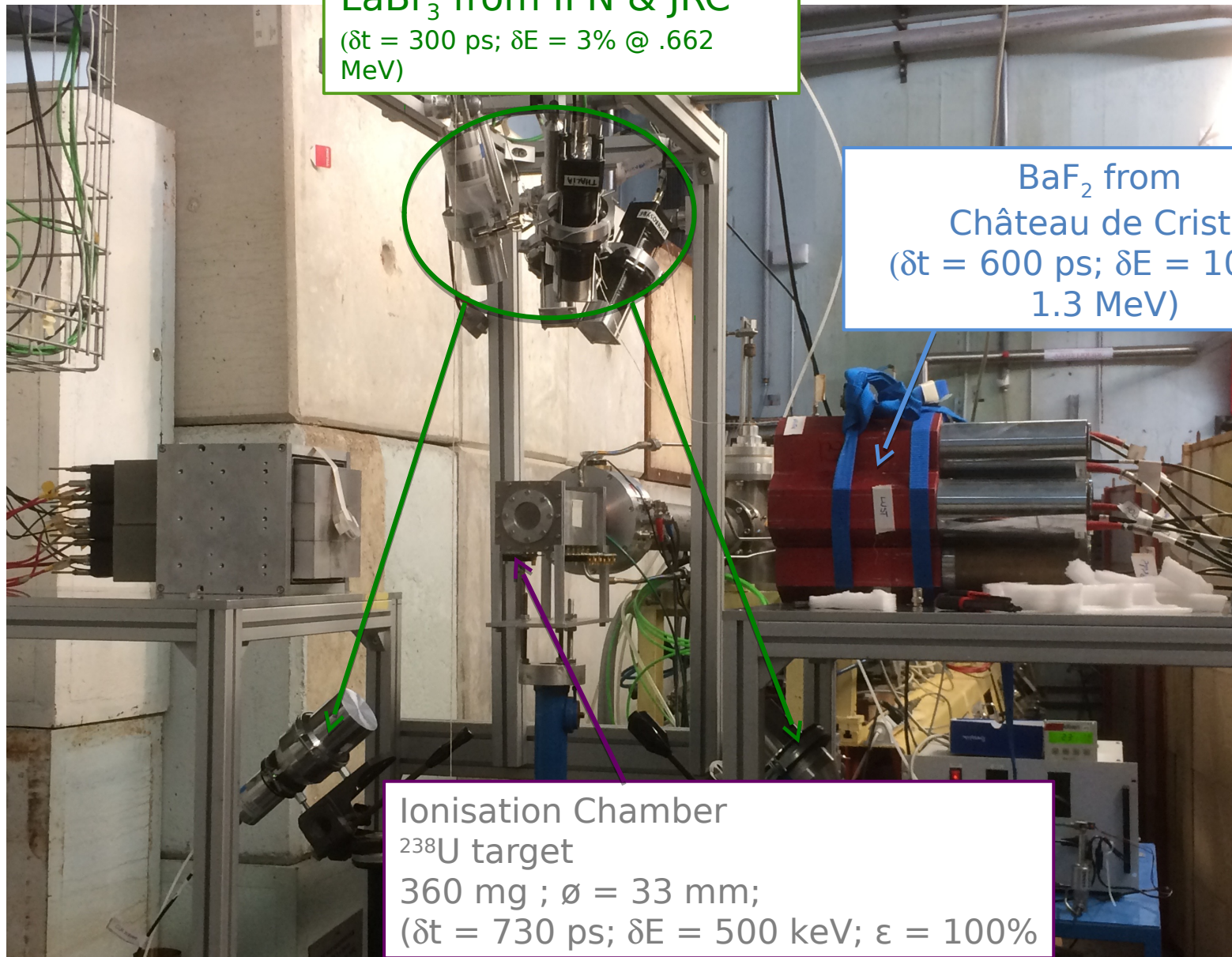
May 29, 2017

L. QI IPNO



Fission- alpha discrimination

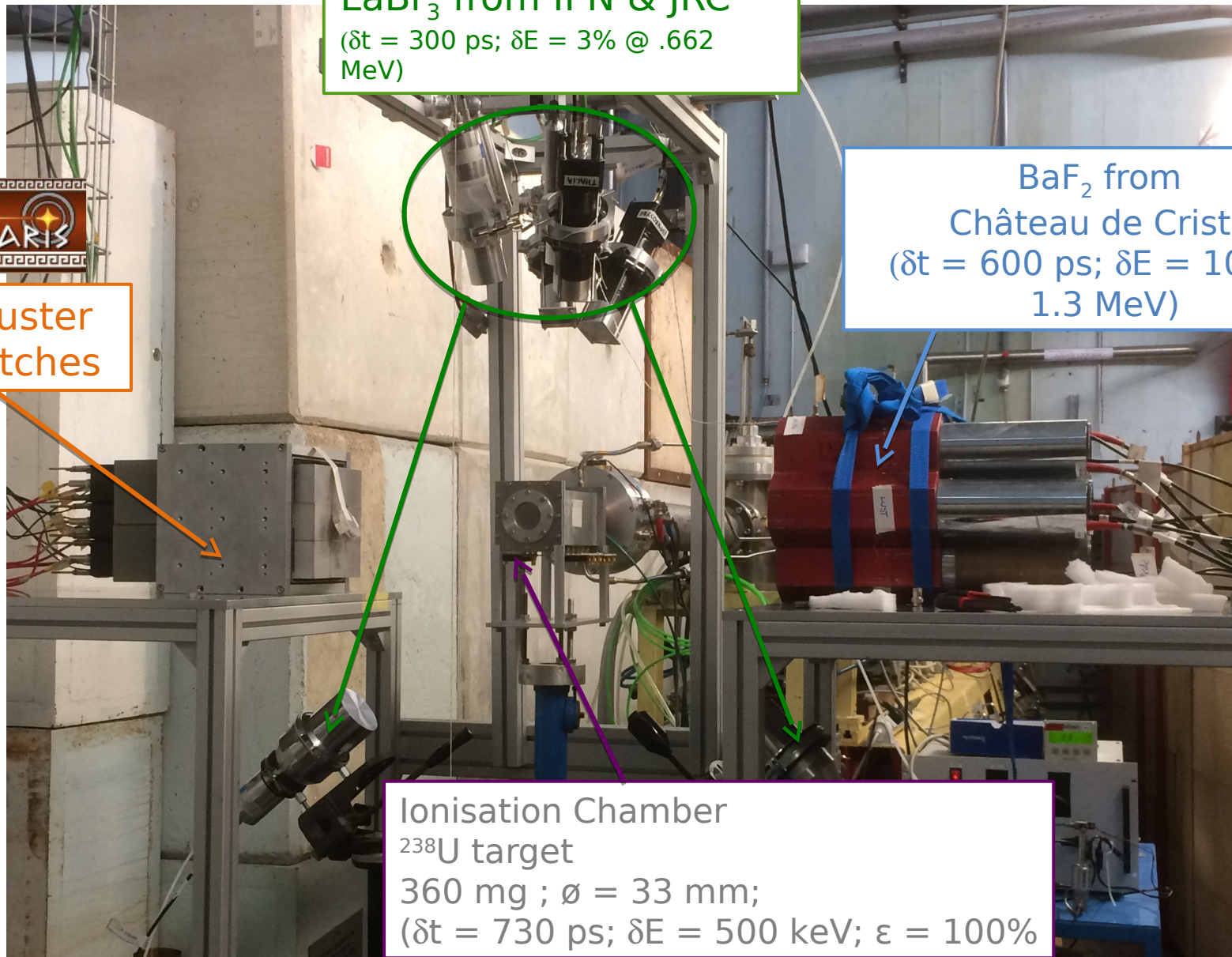




LaBr₃ from IPN & JRC
($\delta t = 300$ ps; $\delta E = 3\%$ @ .662 MeV)

BaF₂ from
Château de Cristal
($\delta t = 600$ ps; $\delta E = 10\%$ @
1.3 MeV)

Ionisation Chamber
 ^{238}U target
360 mg ; $\varnothing = 33$ mm;
($\delta t = 730$ ps; $\delta E = 500$ keV; $\varepsilon = 100\%$)

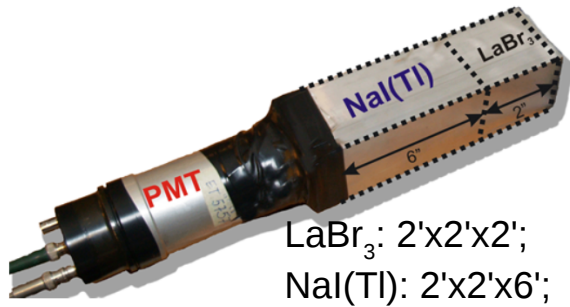


LaBr₃ from IPN & JRC
($\delta t = 300$ ps; $\delta E = 3\%$ @ .662 MeV)

BaF₂ from Château de Cristal
($\delta t = 600$ ps; $\delta E = 10\%$ @ 1.3 MeV)

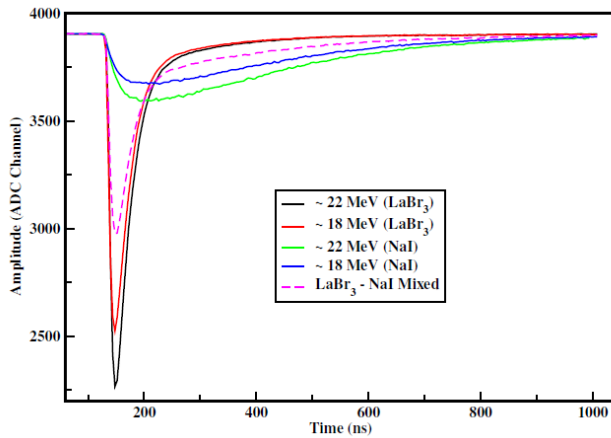
PARIS Cluster
9 phoswitches

Ionisation Chamber
 ^{238}U target
360 mg ; $\varnothing = 33$ mm;
($\delta t = 730$ ps; $\delta E = 500$ keV; $\varepsilon = 100\%$)

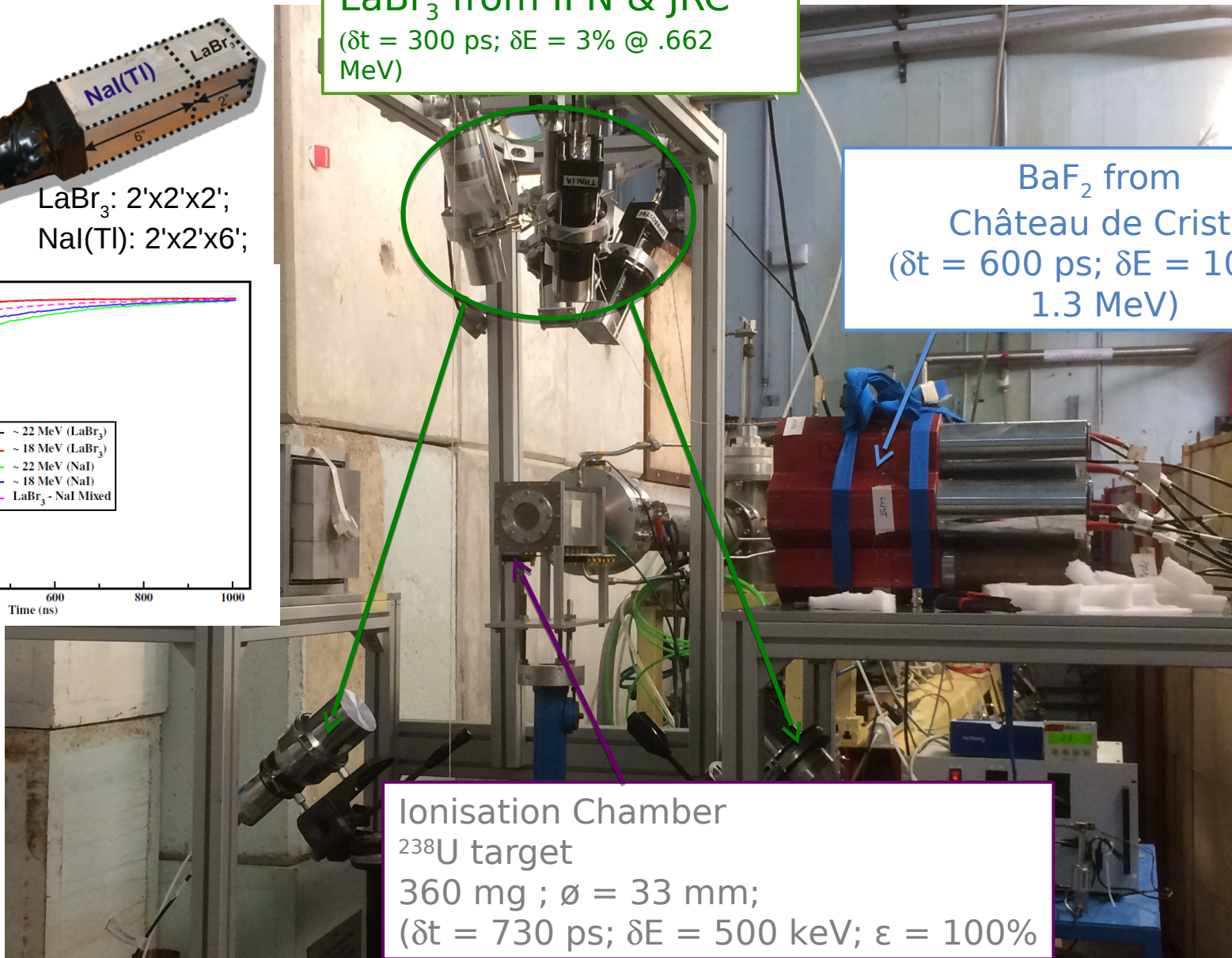


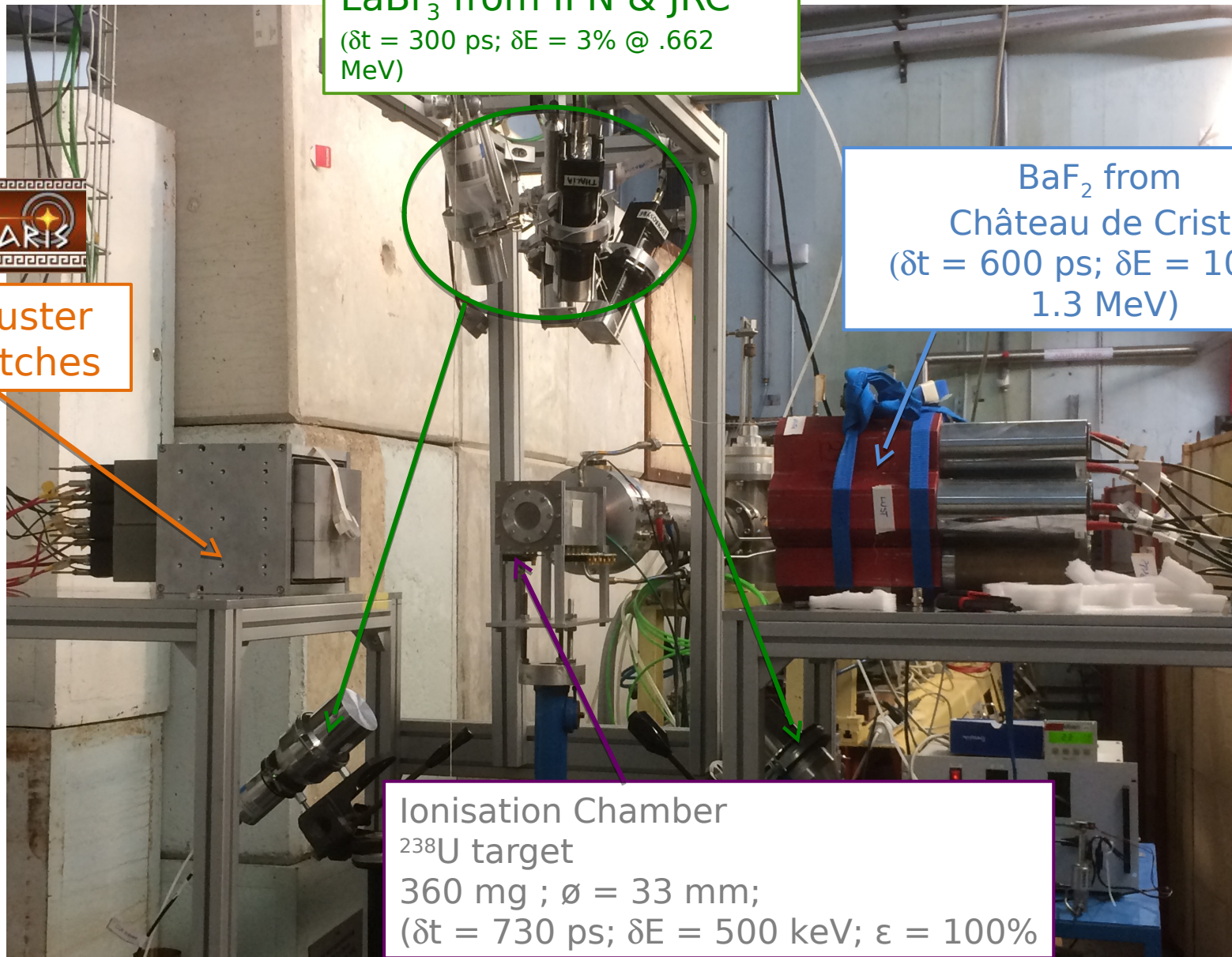
LaBr₃: 2'x2'x2';
NaI(Tl): 2'x2'x6';

LaBr₃ from IPN & JRC
($\delta t = 300$ ps; $\delta E = 3\%$ @ .662 MeV)



BaF₂ from
Château de Cristal
($\delta t = 600$ ps; $\delta E = 10\%$ @
1.3 MeV)





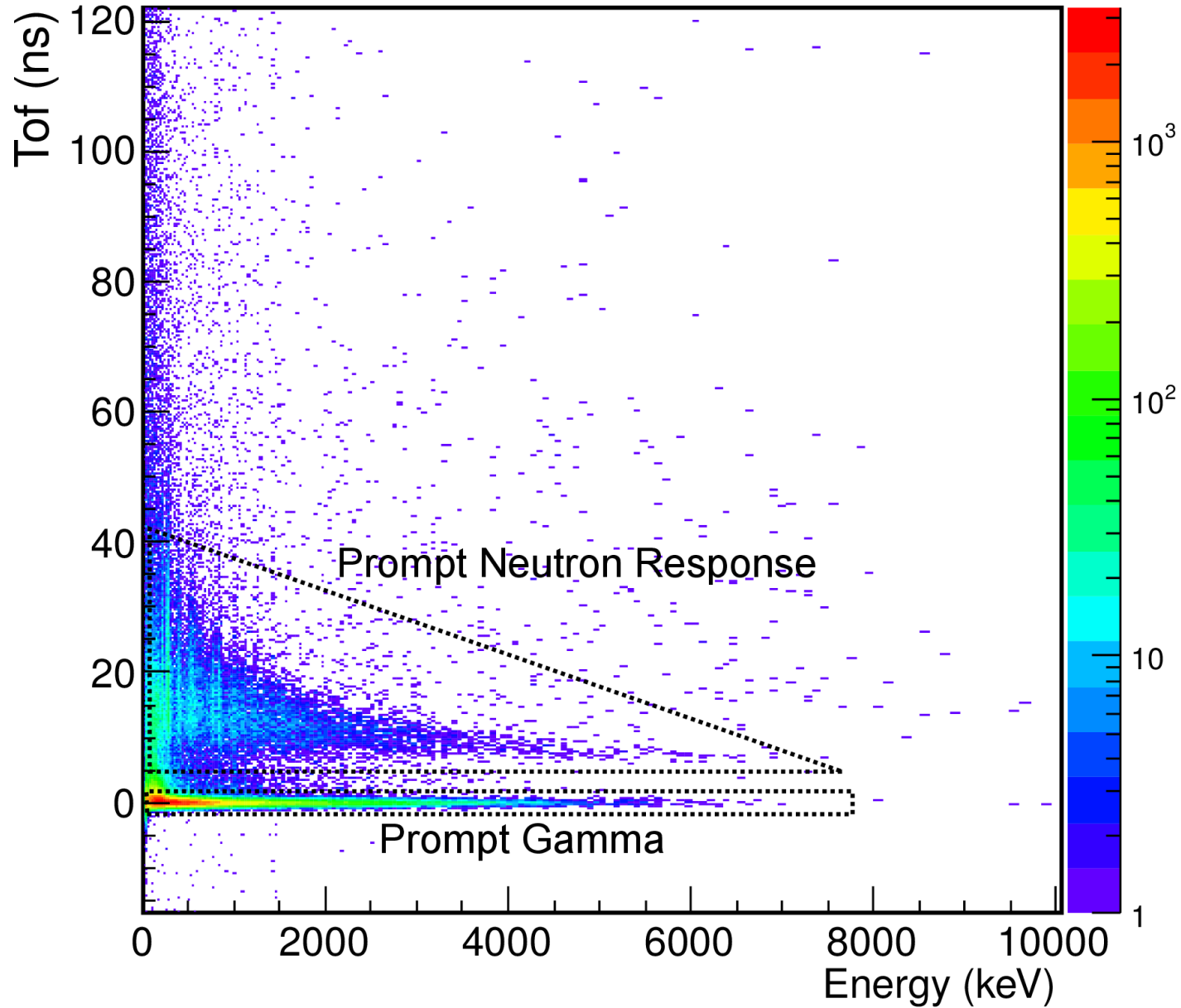
LaBr₃ from IPN & JRC
($\delta t = 300$ ps; $\delta E = 3\%$ @ .662 MeV)

BaF₂ from Château de Cristal
($\delta t = 600$ ps; $\delta E = 10\%$ @ 1.3 MeV)

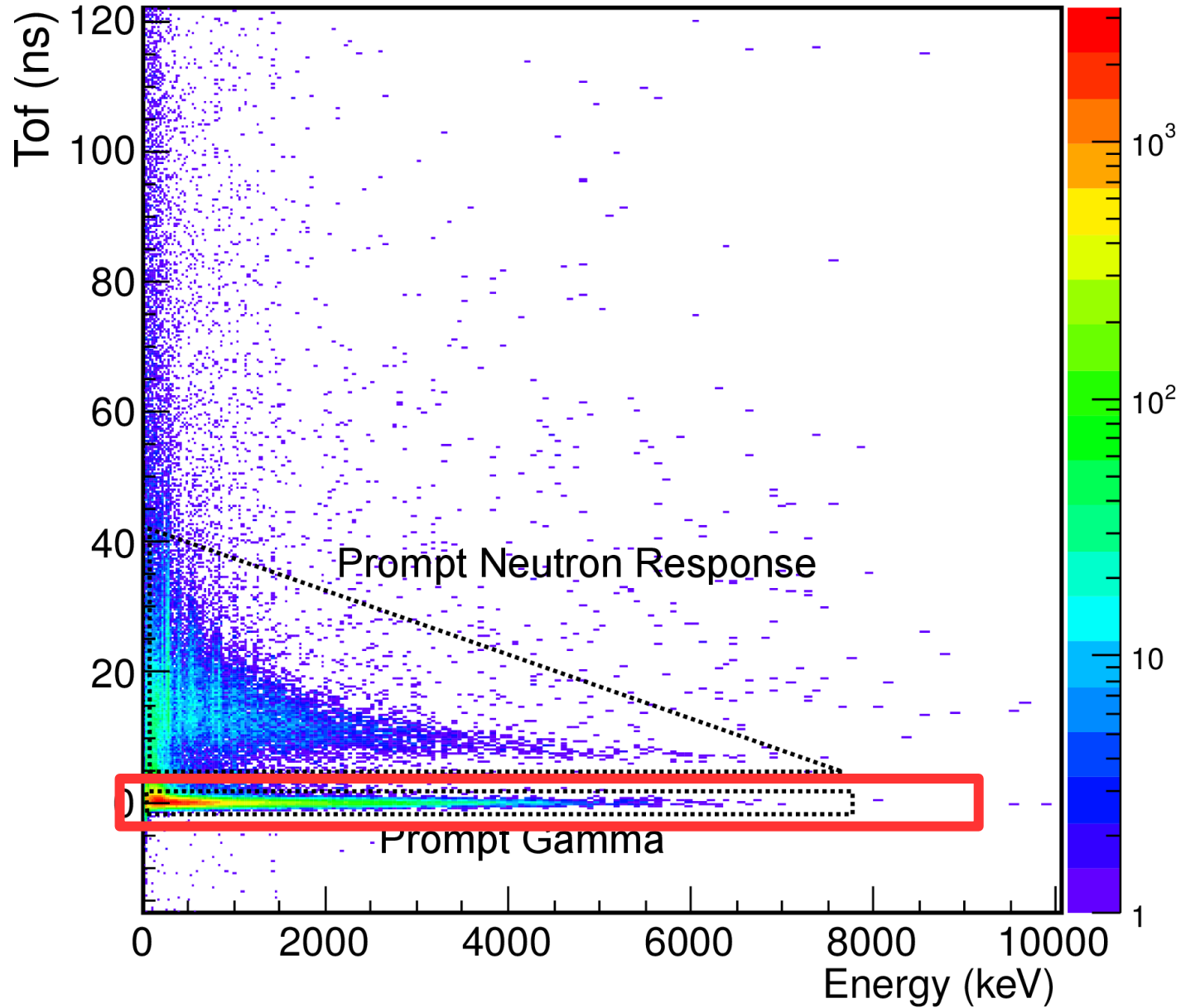
PARIS Cluster
9 phoswitches

Ionisation Chamber
 ^{238}U target
360 mg ; $\varnothing = 33$ mm;
($\delta t = 730$ ps; $\delta E = 500$ keV; $\varepsilon = 100\%$)

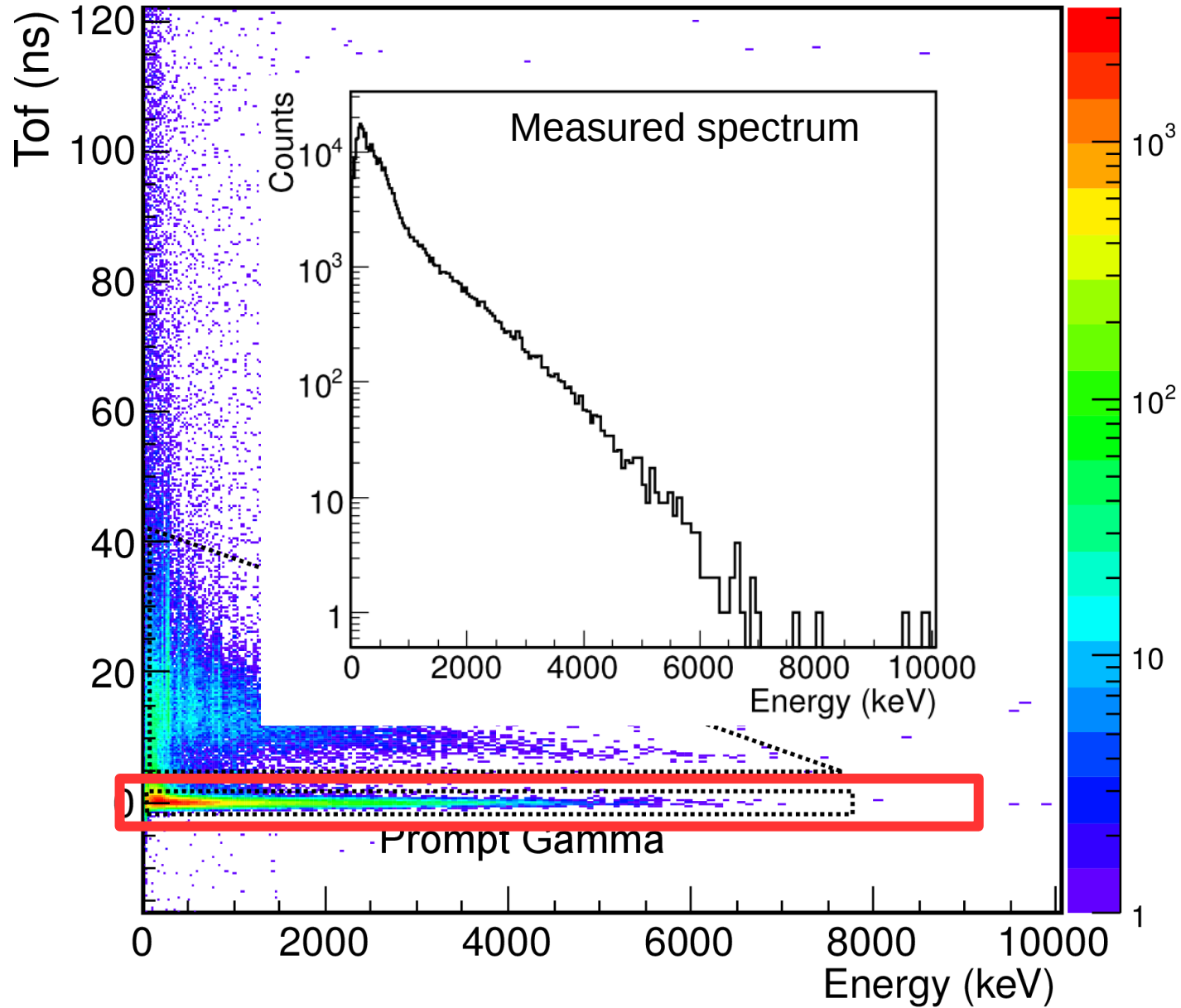
Measured Spectrum: $g(x)$



Measured Spectrum: $g(x)$



Measured Spectrum: $g(x)$



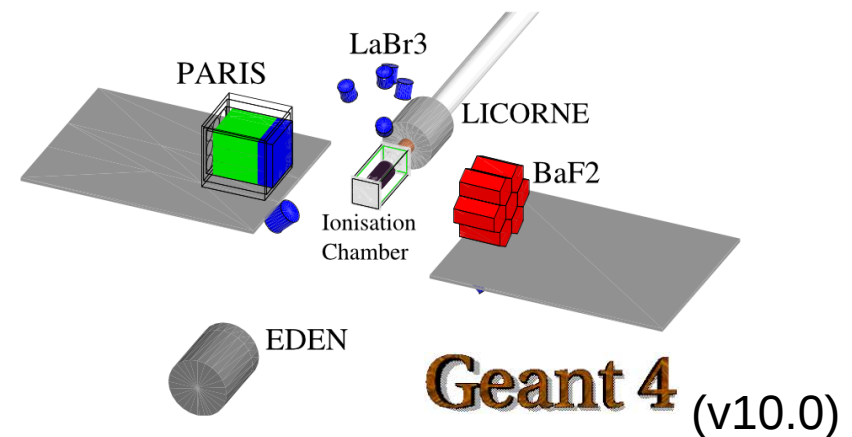
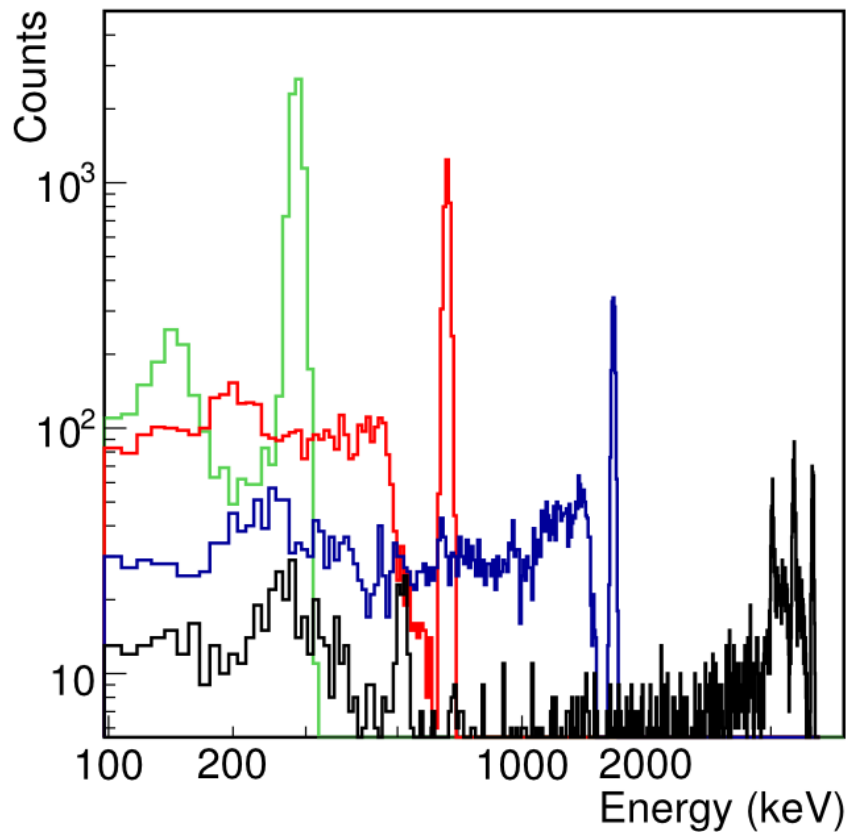
Inverse problem:

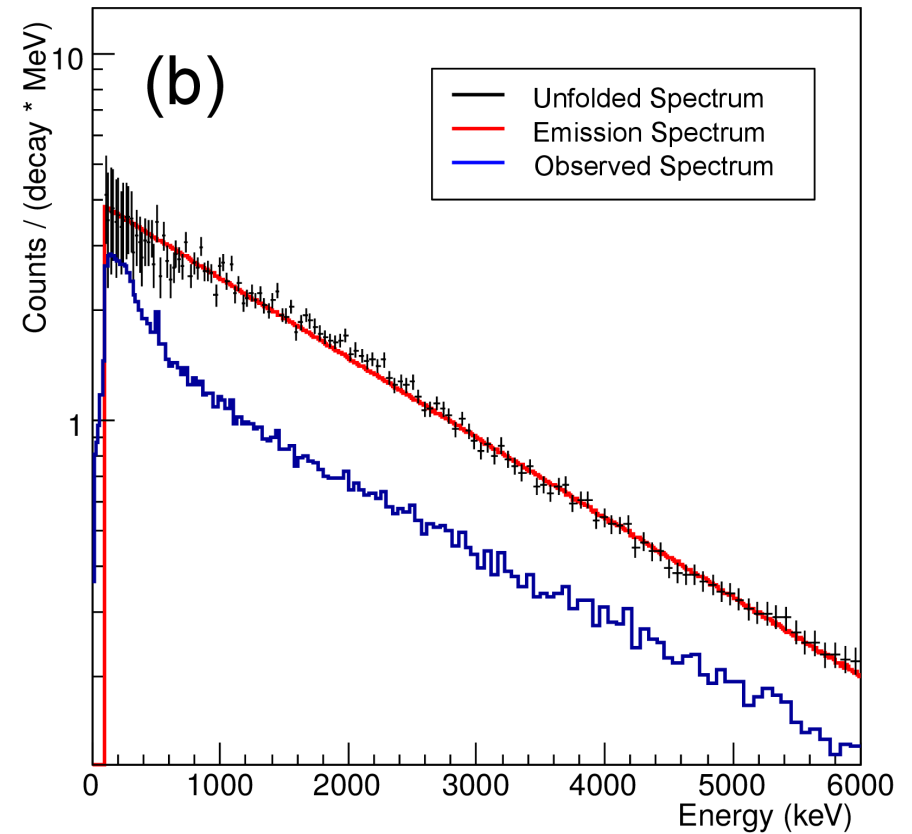
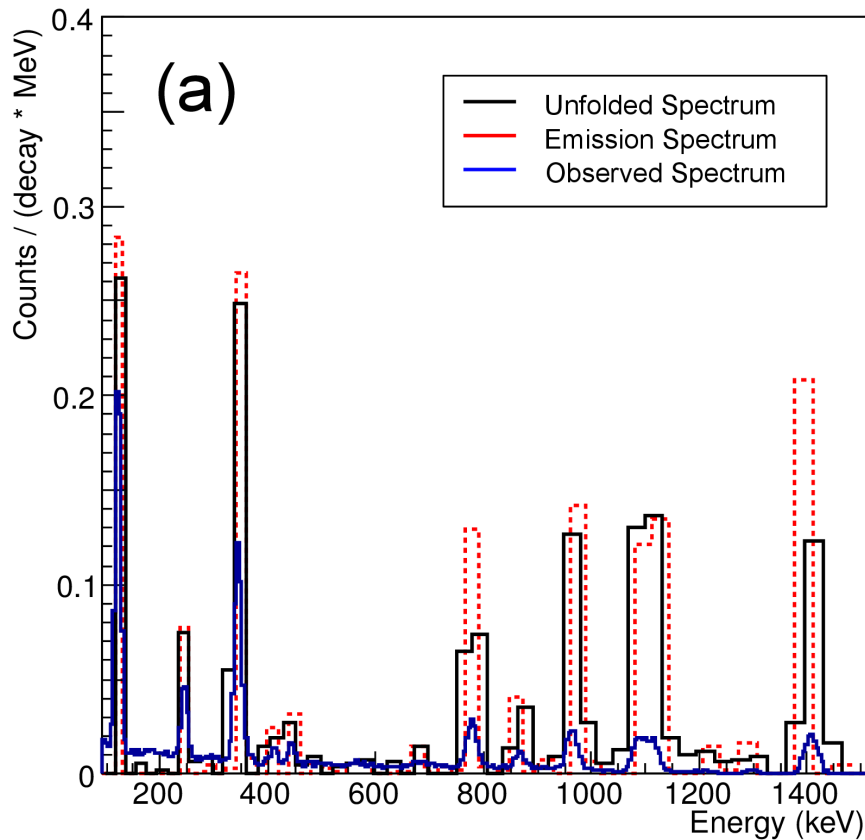
$$g(x) = \int_0^{\infty} R(x, y) f(y)$$

$g(x)$: measured spectrum (observation)

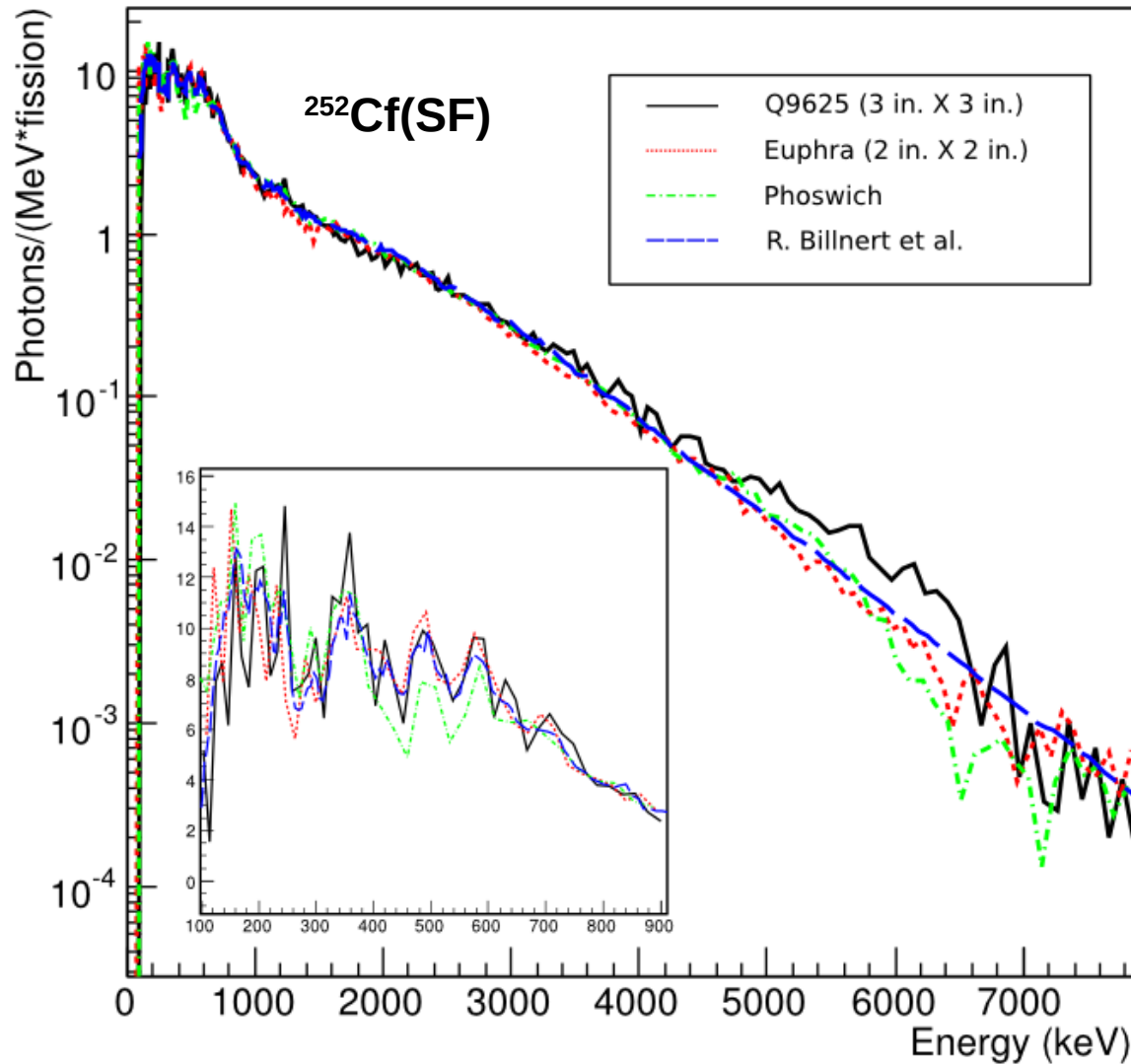
$R(x, y)$: response matrix (simulated)

$f(y)$: emission spectrum (unknown)





Methods	Test1 - discrete distribution			Test2 - continuum distribution		
	Multiplicity M_γ	Total Energy $E_{\gamma,tot}(\text{MeV})$	Average Energy $\epsilon_\gamma(\text{MeV})$	Multiplicity M_γ	Total Energy $E_{\gamma,tot}(\text{MeV})$	Average Energy $\epsilon_\gamma(\text{MeV})$
Bin-by-bin	1.54 ± 0.057	1.09 ± 0.049	0.71 ± 0.041	7.37 ± 0.12	13.09 ± 0.34	1.77 ± 0.054
Matrix Inversion	1.68 ± 0.027	1.19 ± 0.027	0.71 ± 0.020	7.25 ± 0.10	12.89 ± 0.35	1.78 ± 0.055
Linear Iteration	1.65 ± 0.058	1.16 ± 0.024	0.70 ± 0.029	7.28 ± 0.079	12.93 ± 0.073	1.77 ± 0.022
Non-linear Iteration	1.57 ± 0.013	1.11 ± 0.016	0.71 ± 0.012	7.24 ± 0.025	12.83 ± 0.061	1.77 ± 0.010
Regularization	1.59 ± 0.01	1.07 ± 0.015	0.67 ± 0.010	7.27 ± 0.014	13.27 ± 0.040	1.82 ± 0.006
Reference	1.58 ± 0.012	1.11 ± 0.001	0.71 ± 0.008	7.25 ± 0.015	12.86 ± 0.004	1.77 ± 0.001



Results	M_γ	$E_{\gamma,tot}$ (MeV)	ϵ_γ
This work	8.35 ± 0.17	6.65 ± 0.07	0.80 ± 0.02
R. Billnert et al. [1]	8.30 ± 0.09	6.64 ± 0.10	0.80 ± 0.01
Chyzh et al. [2]	8.14 ± 0.40	7.65 ± 0.55	0.94 ± 0.05
ENDF/B-VII.1	7.85	6.13	0.78

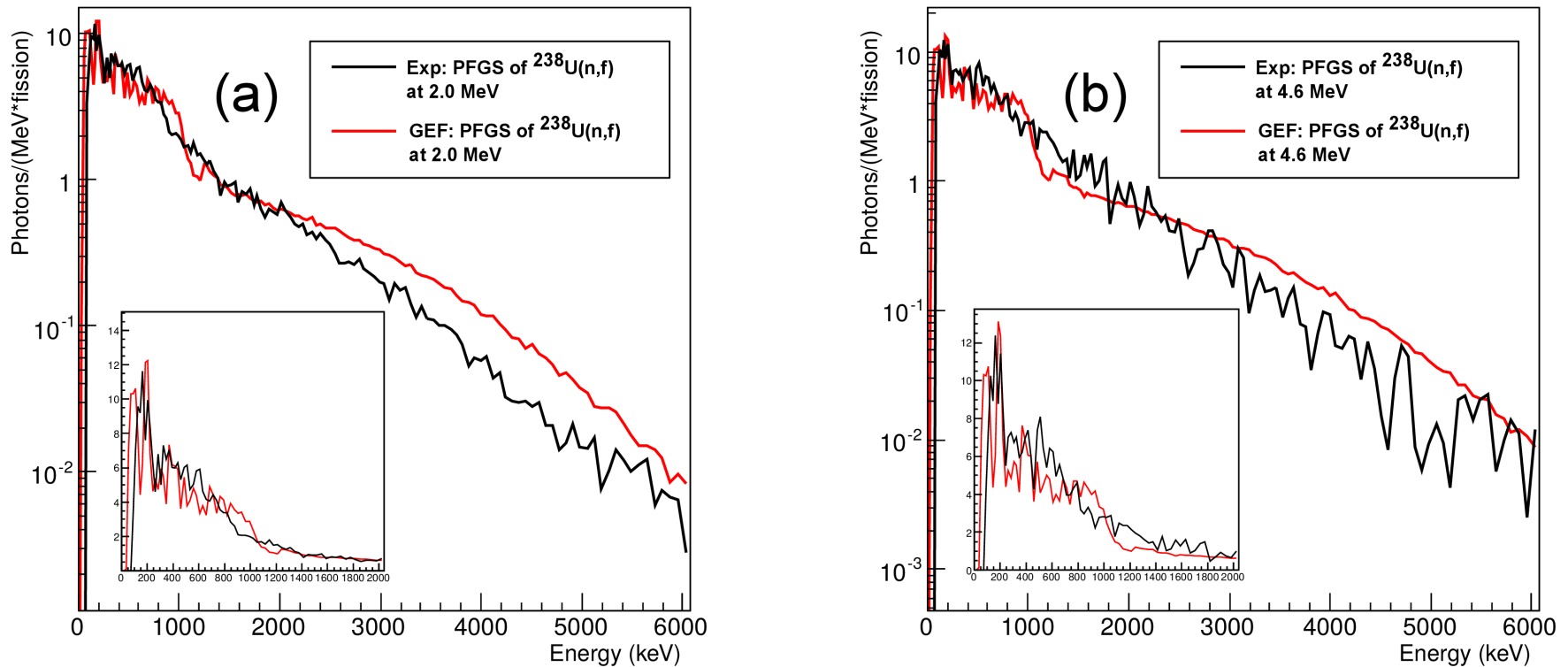


Figure: Comparison between experiments and theoretic calculation.

→ Neither the position of peaks in low energy region nor the slope of the high energy tail agrees with the experimental data. It suggests that the model requires better level density function and gamma strength function.

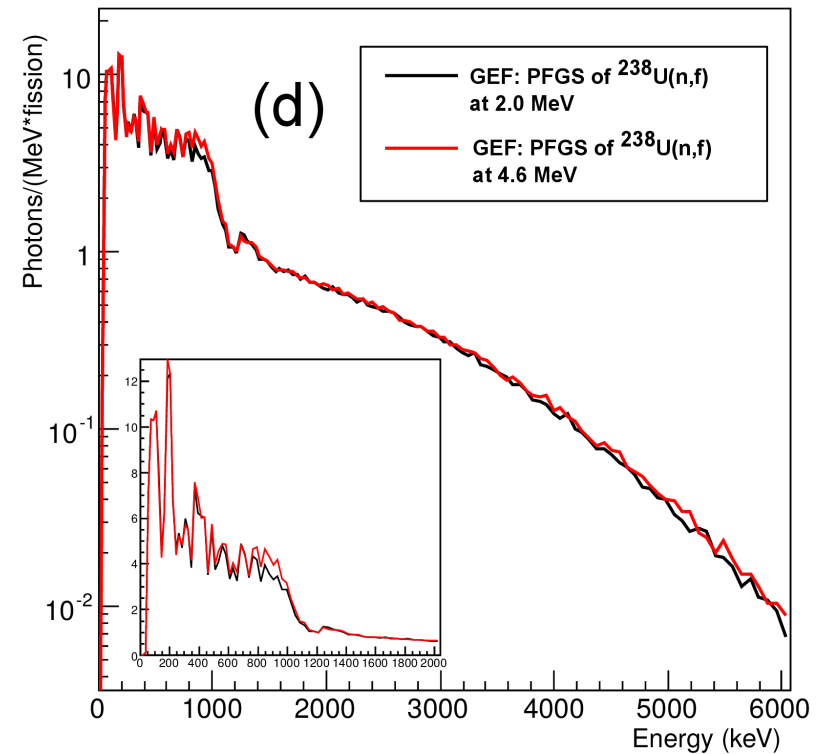
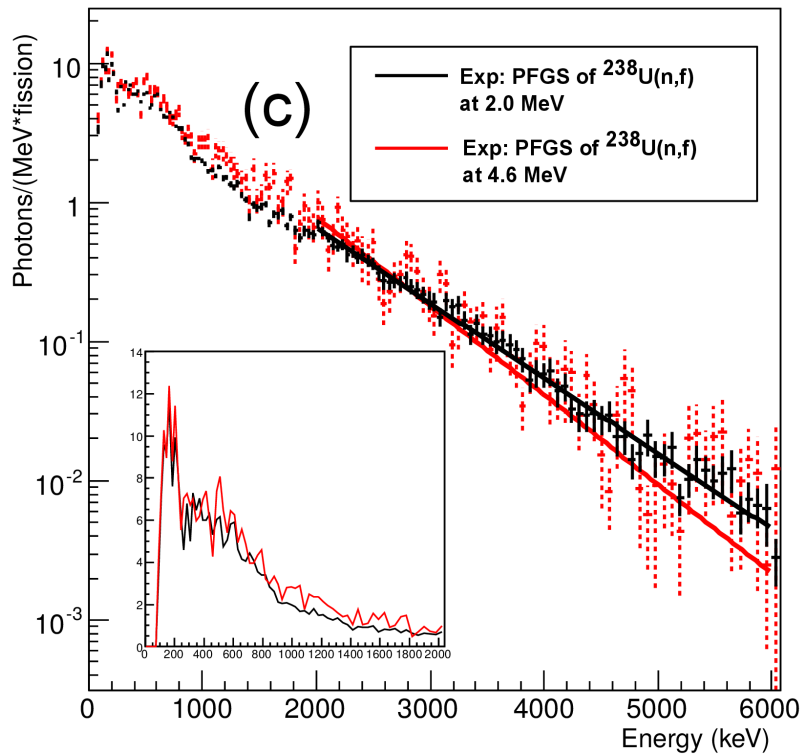
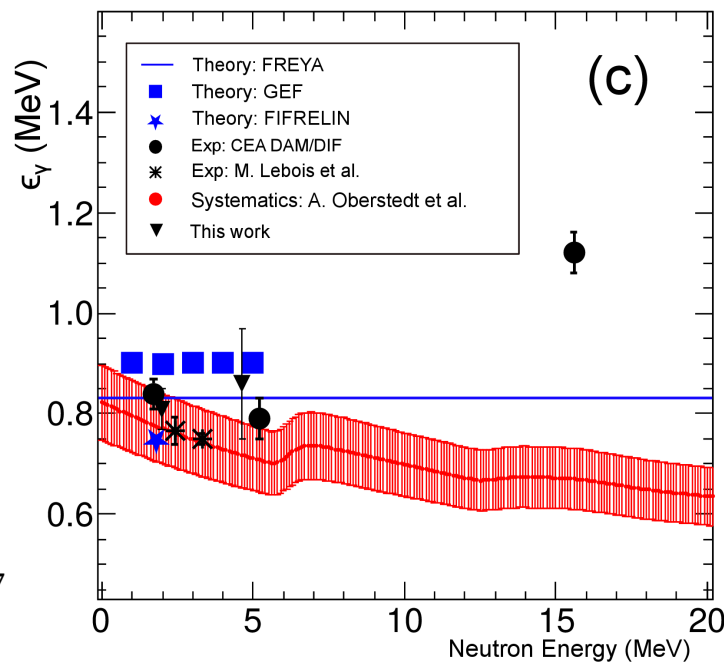
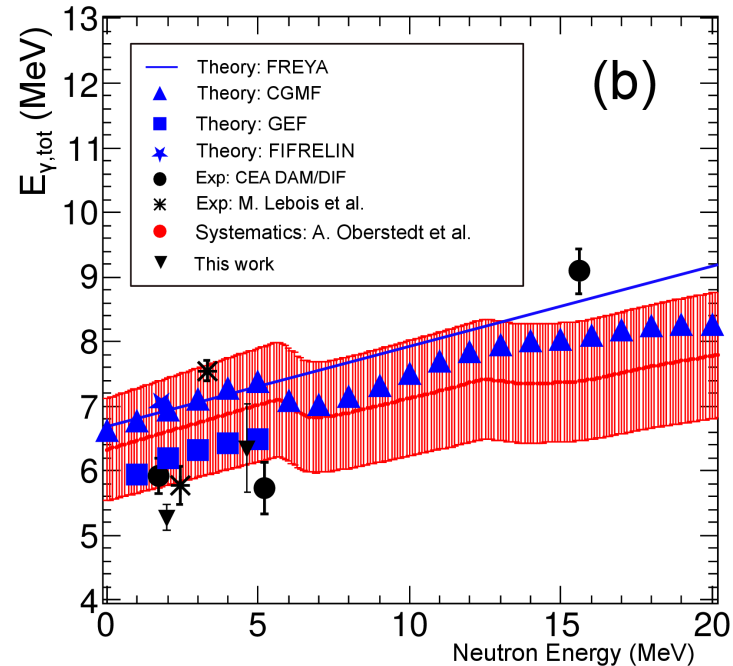
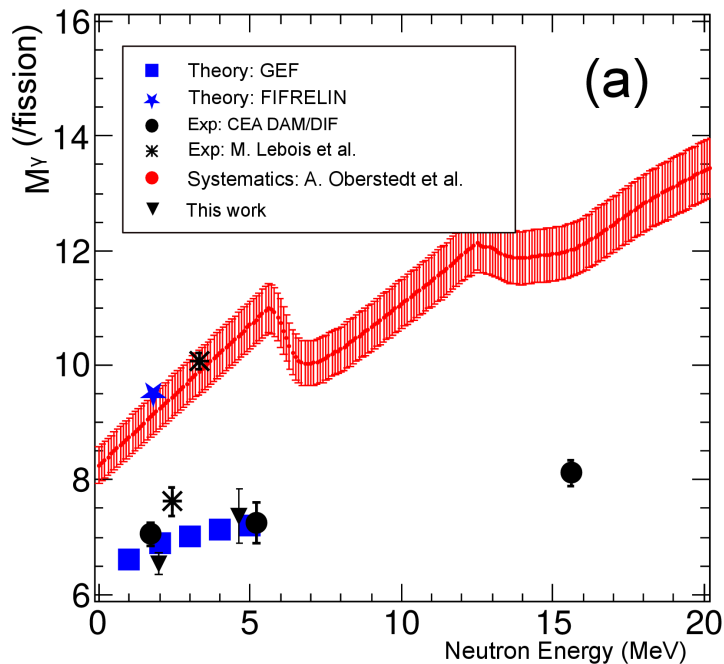


Figure: Internal comparison at different excitation energy.

- The slope change indicated the excitation energy partition, while not obvious in the GEF code calculation
- Also confirms the idea that excess excitation energy is evacuated mainly by neutron evaporation instead of gamma emission.



→ Large discrepancy is observed, especially in terms of the gamma multiplicity;

1. $^{238}\text{U}(n, f)$ is not the origin of the underestimation of gamma heating in reactors;
2. Theory models need to be refined according to the discrepancy appearing in the $^{239}\text{U}^*$ fissioning system;
3. Further physical interpretation is still undergoing.



Thank you for
your attention